Global Scientific JOURNALS

GSJ: Volume 11, Issue 9, September 2023, Online: ISSN 2320-9186
www.globalscientificjournal.com

Rain Attenuation Estimation and Modeling for Terrestrial Microwave and Millimetric Band in Ethiopia

---

By: Meseret Chalachew
Adviser: Dr. Ephrem Teshale

Co-Adviser: Dr. Feyisa Debo

A Thesis submitted to
School of Electrical and Computer Engineering
Addis Ababa Institute of Technology

In Partial Fulfillment of the Requirements for the Degree of Master of Science in Telecommunications Engineering - Telecommunication Network Engineering Track

Addis Ababa University
Addis Ababa, Ethiopia
2022

Addis Ababa University
Addis Ababa Institute of Technology
School of Electrical and Computer Engineering

Rain Attenuation Estimation and Modeling for Terrestrial Microwave and Millimetric Band in Ethiopia

By
Meseret Chalachew
Approved by Board of Examiners

Dr. Ephrem Teshale		
Advisor	Date	Signature
Examiner 1	Date	Signature
Examiner 2	Date	Signature
Program Chair	Date	Signature

Dr. Bisrat Derebssa

Dean, School of Electrical and Computer Engineering

Declaration

I declare that this thesis is a presentation of my own research work and any materials used from any other sources have been clearly identified and acknowledged and it has not been presented to this University or to any other institution for a degree or other qualification.

Meseret Chalachew

Name Signature

Place : Addis ababa
Date of Submission:

This thesis has been submitted for examination with my approval as an advisor.

Dr. Ephrem Teshale

Adviser Signature

Abstract

Researchers and network designers had been encouraged to have a look at communication structures that perform at microwave and millimeter-wave bands for high speed, and dependable wi-fi communication structures. Typically since of blockage within the lower frequency range and expanding demand for huge transmission capacity and excessive channel capability. but, the reliability of radio communication frameworks at the better operation frequency variety may be encouraged by means of different climatic components. precipitation is the major cause of impairment at higher frequency band. Rain attenuation is the prevailing figure within the way loss variety over 7 GHz and 10 GHz in tropical climates causes weakening within the transmitted signal and decrease of the link accessibility. In microwave design rain attenuation parameter using local data in Ethiopian context stays unstudied. Be that as it may, due to the stochastic nature of the rain , it is require for exact propagation estimation due to the reality that over-prediction comes about in expensive over-design, while, under-prediction can result within the lack of quality of the frameworks.

In this paper, long-term rainfall measurements spanning a maximum of 10 years data collected from Ethiopia National Meteorology Agency (ENMA) are obtained for 60 locations and received signal level measurement from Ethio Telecom, to develop rain rate for radio link availabilities between 99% and 99.999% and rain attenuation maps for wireless radio links using Matlab and ArcGIS® software tools and Excel and matlab. The research work has presented a model of 1-minute integration time rain fall rate statistics of different locations in Ethiopia based on as much information as it was possible to gather locally. The shortcoming of some widely used rain rate prediction approaches in relation to Ethiopia's climate has been shown. Hence, a new improved rain rate integration time conversion method, based on 1-minute rain rate data from a specific location, Jimma, has been used with good results. New R0.01 value for Jimma, Bahirdar, Dubti and others rest country in Ethiopia were calculated.

In addition, particular attenuation (dB/km) for both horizontal and vertical polarization is decided as proposed by Worldwide Telecommunication Union (ITU) proposals at chosen frequencies for the arranging of remote systems.Comes about gotten from this approach consolidating both precipitation rate zones and particular attenuation over Ethiopia are displayed as spatial contour maps representations for different ranges of link accessibility. It's conceived that these maps will work as a valuable asset for speedy reference for future link plan estimates, for terrestrial and satellite systems over Ethiopia, East Africa. A comparison look at is finished on those to be had rain attenuation models; The ITU-R model, Crane international model, and also Moupfouma model at unique frequencies and propagation path lengths upheld the exact 1-minute integration time rain rate surpassed at 0.01% of the time-averaged over a length of 10 a long time for each geological area. As a result, the attenuation predicted by new conversion model with ITU-R method has better attenuation estimation than other existing models. It is possible see the clear difference from this result for this specific location.

Keywords: ***Rain rate distribution, conversion factor, contour map, Prediction models, Rain attenuation***

Acknowledgment

First and foremost, praises and thanks to the God, the Almighty, for His showers of blessings throughout my research work to complete the research successfully.

I would like to express my deep and sincere gratitude to my research advisor Dr. Ephrem teshale for giving me the opportunity to do research and providing invaluable guidance throughout this research. His dynamism, vision, sincerity and motivation have deeply inspired me. He has taught me the methodology to carry out the research and to present the research works as clearly as possible. It was a great privilege and honor to work and study under his guidance. I am extremely grateful for what he has offered me. I would also like to thank him for his friendship, empathy, and great sense of humor.

I would like to thank Ethio Telecom for giving me a full scholarship and allowing me to get data for my research. Thank you all ethio telecom staff, friends who motivated, supported, and provided me with your precious ideas. And my special thanks to Ethiopian National Meteorological Agency to providing the necessary data and materials for this study.

I would like to thank Addis Ababa Institute of Technology, School of Computer and Electrical Engineering Department, the instructors, the school dean and the chair person for all the effort that has been put to run this program successfully.

I am extremely grateful to my parents for their love, prayers, caring and sacrifices for educating and preparing me for my future. Also I express my thanks to my sister and brothers for their support and valuable prayers. Special thanks to Feromsa girma, a dear friend at work, without whose persistence I could not have started this altogether.

Contents

List of Figures

List of Tables

Acronyms

ArcGIS Geographic Information System

CCDF Complementary Cumulative Distribution Function

CD's Cumulative Distributions

CDF Cumulative Distribution Function

CV Cross Validation

ENMA Ethiopian National Meteorological Agency

FA2 Factor of Two

FB Correlation Fractional Bias

FSL Free-Space Loss

IDW Inverse Distance Weighting

ITU-R International Telecommunication Union- Radio communication Sector

MAE Mean Absolute Error

ME Mean Error

mm-Wave Millimeter-Wave

LOS Line of sight

PDF Probability Density Function

RMSE Root Mean Square Error

RMSE Root Mean Squared Error

RSD Raindrop Size Distribution

TIN Triangular Interpolation Network

VAR Variance

Chapter 1

Introduction

1.1 Background

The study of precipitation impacts on the terrestrial line of sight paths within the microwave and millimetric wavebands has increased in later a long time. Typically due to the blockage within the lower microwave bands and the require for high capacity communication channels. Frequency bands within the microwave and millimeter spectra are increasingly becoming important to service providers and system planners since of their maximum data-carrying capacity required to match the desires of end-users of wireless communication systems. These bands are projected to supply larger bandwidths, which is important for enhanced network performances, especially in areas of high-speed data transmission and video diffusion[1]. However, the variety of environmental design factors, such as rainfall, atmospheric gas and diffraction fading due to multiple paths, affect wave propagation, leading to signal fading in microwave and millimeter bands [2][3][4]. Among these factors, rainfall is one of the major causes of signal attenuation and network outages at these bands [5][6][7]. The presence of rainfall worldwide results in attenuation of transmission signals in these bands, although the scale of causality depends heavily on climatic and geographic characteristics. Depending on the climate of the considered locale, the rain attenuation gets to be the foremost critical parameter corrupting the execution of signal transmission between line-of sights (LOS) microwave links over a frequency limit[8]. Within the temperate climates, this frequency limit is approximately 10 GHz, whereas inside the tropical climates and in central climate especially, the rate of precipitation on radio links gets to be critical for frequencies as low as almost 7 GHz, since raindrops are bigger than inside the temperate climate[8][9]. For that reason, within the planning of terrestrial line-of-sight systems at microwave and millimeter wavelengths, precise and exact rainfall-rate measurements data are crucial for the correct forecast of rain-induced attenuation on propagation ways.

An appropriate parameter that calculates rain attenuation along radio ways is described empirically through link estimations or anticipated from point precipitation rate, drop-size dispersion, and others. Various authors proposed for the prediction of rain attenuation ,like,[10][11][12][13]. Most attenuation models are based at the accuracy of the total precipitation dispersion at a particular point.

All of these models are planning for the estimation of precipitation attenuation, especially when satisfactory or coordinate measures are not accessible. But by reason of the truth that of the behavior of rain process it is challenging to predict exact behavior of radio waves propagating through rain[14]. Indeed so, over expectation of a propagation impact can result in expensive over-design of a system while,

under-prediction can result in a system that's unreliable[15]. There have been only a limited number of studies, and this area has still not been explored. The research presented in this research aims to bridge this gap by estimating and modeling rain attenuation for terrestrial microwave and millimeter bands. The developed model better estimate the rain attenuation for terrestrial link. Rain being the most fundamental form of precipitation fade mechanism in most part of Ethiopia; the research will try to model and estimate rain attenuation on terrestrial line of sight for Ethiopia.

In Ethiopia, as in many other countries in Africa, rain rate statistics are poorly documented. Thus, the link budget for systems designed in such areas and regions is generally determined on estimation basis. For this study, the Ethiopian National Meteorological Agency (ENMA) has collected 10-year (2012-2020) rainfall rate statistics for 60 different geographic locations in Ethiopia. When reliable long-term local rainfall rate data is available with integration times greater than 1-min,(e.g. Recommendation ITU-R P.530) provides a method for converting rainfall rate statistics with integration times that exceed 1-min to pricipitation rate information with a 1-min integration of time. These precipitation rate information are at that point handled with the 1- minute rain rate information employing a conversion model to anticipate the rain rate and rain-induced attenuation on earthbound line-of-sight links for Ethiopia.

1.2 Statement of The Problem

Radio wave is degraded that are moving through lower air layer since of the existence of air particles. The air gasses and rain both retain and diffuse the radio waves and subsequently corrupt the execution of the microwave radio link. Microwave and Millimeter-wave (mm-Wave) are today's breakthrough frontier for developing remote portable cellular systems, remote local area systems,and individual area systems[16]. In Ethiopia, the data interface reliability is influenced by air particles. Among these air constituents, precipitation is the major cause of impedance at higher frequency bands[17].

Rain is the main cause of communication impairment so, it is challenging to induce a model that enough predicts the dynamic behavior of propagation in rain. Since over-prediction results in expensive over-design, while, under-prediction result within the lack of quality of the frameworks. Precipitation is a random process that shows varieties over radio wave propagation causing changing precipitation attenuation. Variations in radio climatological elements in different regions of the world cause changes in design parameters. As a result, there is a need for exact radio propagation data from different regions of Ethiopia to have proper radio propagation models for terrestrial LOS link in Ethiopia.

1.3 Objectives

In this section the general and the specific objective of the study is described. The general objective lays down the general target of the research work presented herein. The specific objectives give a detailed view of how the research is planned and the type of research problems that have to be addressed on the way to the result.

1.3.1 General objective

The general objective of this research is to estimate and analyze the most suitable rain attenuation prediction model for Ethiopia.

1.3.2 Specific objectives

The specific aims of the research are:

- To obtain precise precipitation rate information for diverse geographical areas in Ethiopia for several years at the 1-minute integration time.
- To determine the cumulative distributions of the rainfall rate for different geographical locations in Ethiopia.
- To determine the rain rate exceeded for 0.01% of the time for each of the locations.
- To compute the particular rain attenuation for the diverse areas based on the accessible rain information.
- To estimate the precipitation attenuation exceeded for 0.01% of the time for diverse climatic zones in Ethiopia using present existing models.
- To define and propose an appropriate rain attenuation model for Ethiopia.
- To develop contour maps for rain rate distribution at different exceedence of time and specific attenuation at different frequency bands in Ethiopia.

1.4 Literature review

Sujan shrestha et al. in [18] proposed Rain attenuation measurements over millimeter-wave bands had been done in South Korea. They displayed the investigations of rain attenuation and precipitation information for three years, in a 3.2 km linked at 38 GHz and 0.1 km linked at 75 GHz. They have been used OTT Parsivel for gathering the rain rate database. They utilized distinctive Forecast models,especially, ITU-R P.530-16, Moupfouma, Abdulrahman,and differential condition method are analyzed. The strength of the research allows to pick out the maximum appropriate rain attenuation model for better microwave bands. They show, interestingly, ITU-R P. 530-16 exceedingly nearer estimation to measured rain attenuation and fewer error possibilities than others prediction models . moreover, the efficacy of the frequency scaling approach of rain attenuation among hyperlinks distribution is likewise defined on paper. in the end, this paper is beneficial for making appropriate concerns in rain attenuation predictions for terrestrial links running at better frequencies. But the main gap in this study were

numbered of sites are not enough to conclude the impact of rain on the region and they did not develop regional contour maps.

HOSSAIN Sakir in [19] proposed Rain Attenuation measurements for Terrestrial radio Link in main cities of Bangladesh. He mentioned that rain rate is higher at Sylhet among the concerned cities. During his analysis he has concluded that specific attenuation of the stated towns stays very near up to twenty-five GHz, observed by significant distinction for better frequencies.He additionally discovered that the horizontally polarized signal is greater suffering from the precipitation than the circularly and vertically polarized signal. hence, the usage of vertical polarization within the excessive rain region like Sylhet is extra cost-effective . Finally, he has encouraged all of the predicted information may be used to use the frequency variety method for decreasing the impact of rainfall on microwave conversation. But the main gap of the study were he tooks not enough sites to conclude the impact of rain distribution on region and also comparison of different alternative model and validation was not done.

F. D. Diba in [17] proposed the precipitation rate distributions for different geographical area in Ethiopia were determined at the 15-minute sampling rain rate. He used R-H model for time conversion. In addition, the precipitation rate contour maps at 0.01% exceedance are advanced in Ethiopia. He was using the ITU-R model to analayze rain attenuation by various frequencies and separations. He concludes that the weakening for shorter interface paths is more prominent stricken by precipitation than longer distance since of the non-uniformity of rain dispersion over the hyperlink. During his analysis, he was concluded that the attenuation of precipitation rate is the most noteworthy in Bahirdar, taken after by Jimma, diredawa, Mekele, Negele Borena and, Kombolcha, AddisAbaba, Adama, Arbaminch, least in Dubti. Many researchers have studied the rain effects on radio links in different tropical [20][21][22][23][24][25][26]][27][28][29]. Be that as it may, numerous tropical and central African districts have not been enough considered.

Finally, for a precipitation attenuation show to precisely predict rain weakening beside a terrestrial radio interface, an exact expectation of the precipitation rate measurements, and the drop-size dispersion, must be promptly accessible for the specific climatic rain zone in which the forecast is to be made. That's why the rain weakening demonstrate predicted in one climatic region may not be satisfactory or substantial for the other climatic region. Numerous studies have been carried out in calm climates, but small has been detailed almost tropical and equatorial climates, in which Ethiopia falls; subsequently, this study to fill the gap.

1.5 Methodology

In order to have a better understanding of this thesis work, different related literatures, journals, and books on rain attenuation predication have been reviewed. Relevant materials for rain attenuation prediction models are also referred. Moreover, Ethio telecom process manuals and link design documents are also consulted to understand the estimation and modeling of rain attenuation. This thesis was performed by using the following methods:

- The thesis work started with a literature review to understand more the purpose of the research and then familiarize with the available related research works and necessary data for the study has been identified.
- Rainfall data collection from Ethiopia national meteorological agency and microwave link budget from Ethio telecom.
- Statistical data analysis and modelling using MS-Excel and Matlab.
- During data analysis, comparison and validation have been done to estimate the rain rate distribution and attenuation
- Interpolate the missing geographical area using different interpolation techniques (IDW and Kriging) and develop contour map using ArcGIS software

1.6 Scope and Limitation of the study

1.6.1 Scope of the study

The research is basically focused to develop a contour map of rain rates over terrestrial radio links in Ethiopia based on regionally measured rain information. The studies is achieved to estimate and analyze the maximum appropriate rain attenuation prediction model for Ethiopia.

1.6.2 Limitation of the study

This thesis is limited owing to lack of 1-min integration time rain rate data for locations other than Jimma, rain rate conversion procedure based on 1-min rain data from Jimma has been used. Although this approach produced better estimation results than some global models, it still needs to be refined with local rain rate measurement data.

1.7 Contributions of the research

The significant contributions of this research work are listed as takes after:

- As has been mentioned above, this proposed work could be a further asset in this study area.

- it's far essential to realize the atmospheric impairment, particularly the precipitation attenuation impact of the microwave link designer. for that reason, the end result of this proposed work can be taken as input before making design to install microwave links in Ethiopia.
- The end result of this research could be beneficial for microwave communication researcher

1.8 Organization of the Thesis

Thesis is prepared in the following way : the first chapter presents the background or introduction, problem statement, objectives, methodology, literature reviews, contributions, and scope and limitations of this thesis are described in this chapter.

Chapter two covers the background of rain effect on microwave and rain attenuation model. In addition, Spatial interpolation methods for calculating rainfall using ArcGis software are discussed in this chapter.

In chapter three are explained the methodology part for the research that have done, rainfall Data Measurement, Processing and modeling over microwave and millimetric bands.

chapter 4 present discuss the end result of the simulation outcomes and compare the simulation outcomes to other current models inclusive of ITU, Mouphuma, and global crane and discussion of the outcomes are defined.

chapter 5 covers the conclusion and recommendation of the thesis.

Chapter 2

Rain Effect on Microwave Propagation

Several essential parameters that influence the spread of electromagnetic waves within the atmosphere like clouds, mist, raindrops,and vapor. OThe speediest development in remote systems has driven to the saturation of the lower frequency groups (1-10 GHz). Particularly inside the region 30-100 GHz the exceptionally reality has moved emphasis to the upper frequency range. Indeed so, climatic impacts, primarily rain, are a prevailing reason of signal degradation at microwave and millimeter bands, which finally ends up in network outages. precipitation attenuation is noticeable from propagation frequencies over 10 GHz inside the zone, whereas within the tropical weather, its impact is felt from 7 GHz[30].while a microwave or millimeter-wave signal passes via a wet medium, the signal energy substantially weakens because of the impact of diffusion and absorption raindrops at different amplitude and phase component. Furthermore, rain droplets change the polarization of the transmitted signal, coming about in depolarization impacts at the recipient. Microwave network plan needs information on precipitation attenuation, and depolarization to fulfill the standard and unwavering quality determinations for ideal system capability [31]. In practice, the parameters of precipitation rate and raindrop measure are explored to reinforce the understanding of precipitation impacts over remote systems.

2.1 Earth's Atmosphere

The atmosphere is assumed as a mixture of gases and vapors surrounding the planet. It is divided into four main layers keep with the variability of the gradient with altitude. These layers are usually referred to as the troposphere, stratosphere, mesosphere and thermosphere. The troposphere goes to be the maximum location of interest for this study due to the very truth that it's far a place of excessive radio-climatological instability because of its ground proximity and consequently the unfettered outcomes of the natural surroundings on wave propagation in its area [32] The consequences of precipitation on radio emission propagation growth with working frequencies, mainly above 7 and 10 GHz. The troposphere may increase from the bottom surface to an altitude of about 10 km at the poles and 17 km at the equator with some variation due to weather. It is the thinnest and also rock bottom layer, the warmest and also the wettest, but also the foremost dense with 72% of the entire mass of the atmosphere. The troposphere is typically thought of as the zone of weather since it's where all weather takes place. It is the world of rising and falling packets of air. The atmospheric pressure at the very best of the troposphere is simply 10% of that at sea level. On average, the temperature falls with height during this layer which was given in figure(4.11) below[33].

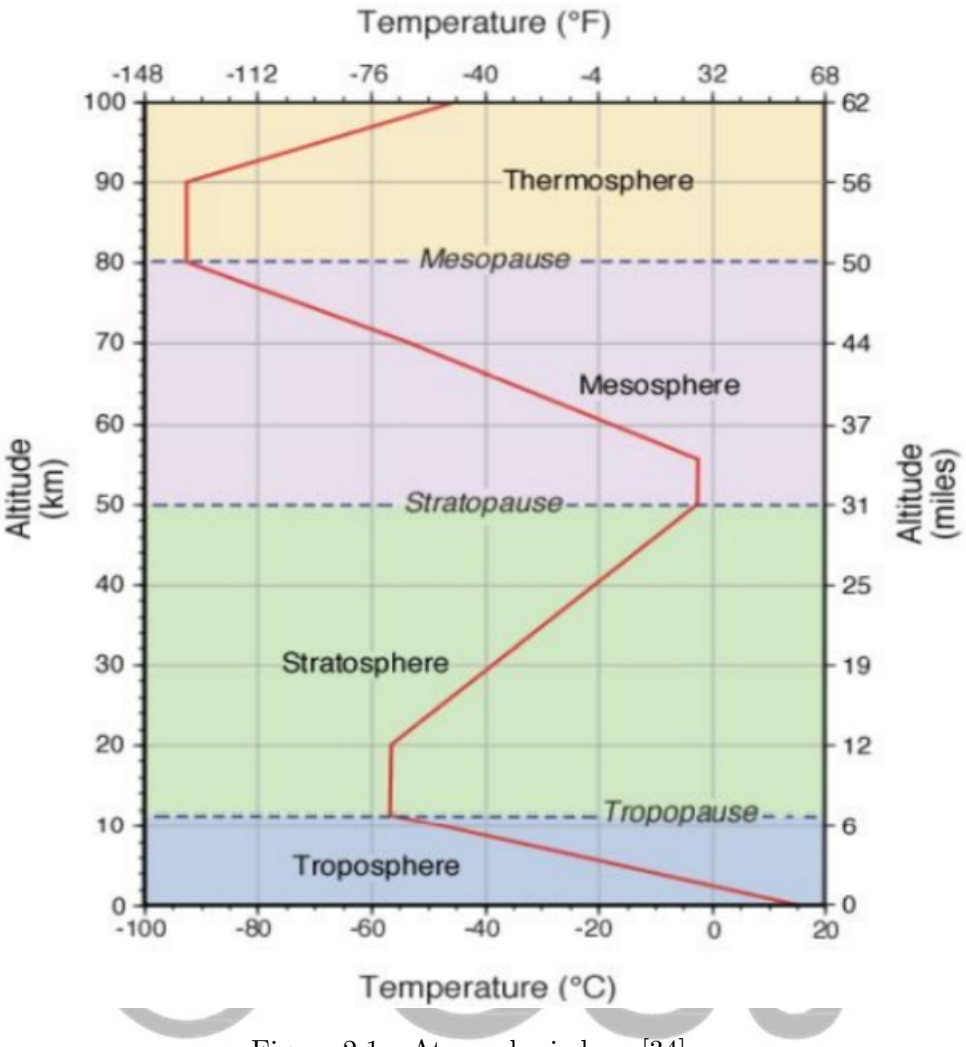

Figure 2.1: Atmospheric layer[34]

2.1.1 Effect of troposphere on terrestrial radio path

The troposphere has numerous effects on terrestrial radio paths such as [35]:

- Attenuation caused by atmospheric gases (generally oxygen and water vapor) and hydro-meteors (rain, fog, hail, snow, mist, Clouds...).
- Alteration inside the beam path shape which ceases to be a straight line and gets to be bended, in reaction to the changes within the refraction index along the path.
- introduction of privileged instructions for wave propagation which allow signal to accomplish distances larger away than might probable with out environment.
- Considerable fluctuations in the amplitude of the received signal because of the existence of different signal path.

- Diffusing due to abnormalities within the higher layers of the troposphere, which empower signals to reach very large separations (a couple of kilometers) and may be utilized to supply troposcatter links.

2.1.2 Effects of precipitation on microwave propagation

The foremost critical impacts of hydrometers on microwave propagation are [8]:

- Attenuations
- Scattering
- De-polarization
- scintillation

2.2 Rain rate distribution

To decide the complete path attenuation, the microwave path loss due to rain weakening must be included to the free-space loss (FSL) whereas considering the expected rain rates. The rain rate is normally measured in mm in keeping with hr. in line with, rain at a rate of one hundred mm (four inches) according to hour or more is taken under consideration as heavy rain. The rainfall rate is typically depending on size(form) of the raindrops. The direction loss generally varies with each the raindrop size distribution (RSD) and rain rate. moreover, the rainfall rate profile isn't always uniform. furthermore, the dimensions of the rain cell (the region occupied through the rain) is taken into consideration as it lies in the direction of the microwave hyperlink. The heavier the raindrops, the smaller are the rain cells. Rainfall can be a time-varying random technique variables over numerous locations of the sector[36]. The dispersion of precipitation rate is utilized to know its impact on radio emission propagation. The critical parameter for rain attenuation is R0.01 gotten from the total dispersion of precipitation rate at 0.01%-time exceedance.

Numerous authors have conducted investigate on the forecast of rain fading, as point by point in [37][38][39]. Most authors proposed models for the expectation of rain attenuation, especially in circumstances where fulfillment estimations are inaccessible. Because of the stochastic nature of rain technique in time and area, it's far hard to get a model that thoroughly predicts the dynamic conduct of rain. However, there may be a demand for accurate propagation estimation because of the very reality that over-prediction finally ends up in expensive over-layout, at the same time as under-prediction can also bring about the unreliability of the structures.

Efforts are made first of all by using the ITU-R 837[40] then via[37] to categories the sector into rain climatic zones to extend the present propagation statistics to a broader range. Those models have, but; ended in plenty inaccuracy in tropical and equatorial areas due to the very truth that almost all

the recorded dataset became developed for temperate area. It discovered that the existing ITU-R rain attenuation estimation technique is not as particular for the tropical sector as it has been determined inside the Temperate area.

In line with ITU-R P 837 [41] the planet is split into zones of world rainfall rate relying on experimental measurements from diverse regions of the world. The classification of the world into 15 rainfall climate zones at different percentages of time exceedance. Accordingly, the important parameters for the determination of rainfall rate for the location into account at any percent of exceedance are longitude and latitude. When ITU-R P 837-1 recommendation, Ethiopia has 4 rainfall weather zones particularly, C, D, E, and J. but, the ITU-R classifications are not necessarily enough designations[42]. From this study, the rainfall rate values at distinct percentages of time for diverse places of Ethiopia don't correspond to ITU-R classification that are expressed in table(2.1)

Table 2.1: Rainfall intensity (mm/h) exceeded at different percentages of time for ITU-R rain climatic zones ITU-R 837-1 [41]

%	A	B	C	D	E	F	G	H	J	K	L	M	N	P	Q
1.0	0.1	0.5	0.7	2.1	0.6	1.7	3	2	8	1.5	2	4	5	12	24
0.3	0.8	2	2.8	4.5	2.4	4.5	7	4	13	4.2	7	11	15	34	49
0.10	2	3	5	8	6	8	12	10	20	12	15	22	35	65	72
0.03	5	6	9	13	12	15	20	11	21	23	33	40	65	105	96
0.01	8	12	15	19	22	28	30	32	35	42	60	63	95	145	115
0.003	14	21	26	29	41	54	45	55	45	70	105	95	140	200	142
0.001	22	32	42	42	70	71	65	53	55	100	150	120	180	250	170

Crane [37] categorized the earth into eight zones, designated A to H with varying amounts of dryness to wetness. Label H is the tropical wet while A implies arctic dry. Using measured datasets, there were differences in rainfall rate at lower percentages of exceedance that leads to the formation of more designations. D zone was then classified into D1- D3, where D1 and D3 stand for driest and wettest seasons respectively. Additionally, this zone of rainfall rate world map gave further designations of B region such as B1 and B2.

Table 2.2: Rain rate (mm/h) exceeded for different percentages of the year [6]

%	A	B	B1	B2	C	D1	D2	D3	E	F	G
1.0	0.2	1.2	0.8	1.4	1.8	2.2	3.0	4.6	7.0	0.6	8.4
0.5	0.5	2.0	1.5	2.4	2. 9	3.8	5.3	8.2	12.6	1.4	13.2
0.3	1.1	2.9	2.2	3.4	4.1	5.3	7.6	11.8	18.4	2.2	17.7
0.2	1.5	3.8	2.9	4.4	5.2	6.8	9.9	15.2	24.1	3.1	22.0
0.1	2.5	5.7	4.5	6.8	7.7	10.3	15.1	22.4	36.2	5.3	31.3
0.05	4.0	8.6	6.8	10.3	11.5	15.3	22.2	31.6	50.4	8.5	43.8
0.03	5.5	11.6	9.0	13.9	15.6	20.3	28.6	39.9	62.4	11.8	55.8
0.02	6.9	14.6	11.3	17.6	19.9	25.4	34.7	47.0	72.2	15.0	66.8
0.01	9.9	21.1	16.1	25.8	29.5	36.2	46.8	61.6	91.5	22.2	90.2
0.05	13.8	29.2	22.3	35.7	4.4	49.2	62.1	78.7	112.0	31.9	118.0
0.003	17.5	36.1	27.8	43.8	50.6	60.4	75.6	93.5	130	41.4	140.8
0.002	20.9	41.7	32.7	50.9	58.9	69.0	88.3	106.6	145.5	50.4	159.6
0.001	28.1	52.1	42.6	63.8	71.6	86.6	114.1	133.2	176.0	70.7	197.0

2.3 Rain rate integration time conversion

During the plan, arranging, execution of terrestrial, and satellite links, satisfactory data on rain attenuation because of precipitation is vital for the area under consideration [43][44]. Assurance of rain attenuation depend upon the rain rate, volume density, and raindrop estimate and shape. Rain attenuation are frequently anticipated by collecting and analyzing information over a period of time. There's all around acknowledged that for exact forecast of precipitation attenuation, rain information with lower examining time is critical. In this manner, recorded precipitation information at one minute or lower integration time are often applied for compelling radio links plan. Agreement with ITU-R [42] forecast of rain attenuation requires precipitation rate at an integration time of 1 min. In any case, 1 min integration time rain information is uncommon in numerous districts of the world. Due to this reality that drive the radio system engineers and planner to utilize a rain rate conversion strategy.This conversion strategy changes over precipitation rate from the higher integration times accessible inside the precipitation information set to the ITU-R suggested one-minute integration time.

In radio emission prediction methods, an integration time of 1 min is utilized. That is often due to the fact rainfall rate measured with excessive-resolution rain gauge, say 1-2 min time decision will solve the tiny however critical rain cells due to the fact longer averaging instances will pass over the height-rain-rate values.

Consequently, 1-min aggregation or averaging time may be a sensible compromise. Since eliminates the fluctuations due to the measurement method, but keeps up the crucial geophysical variations. Longer integration time hides longer rain rate that is why different researchers employed on fast rain gauge(below 10 sec).

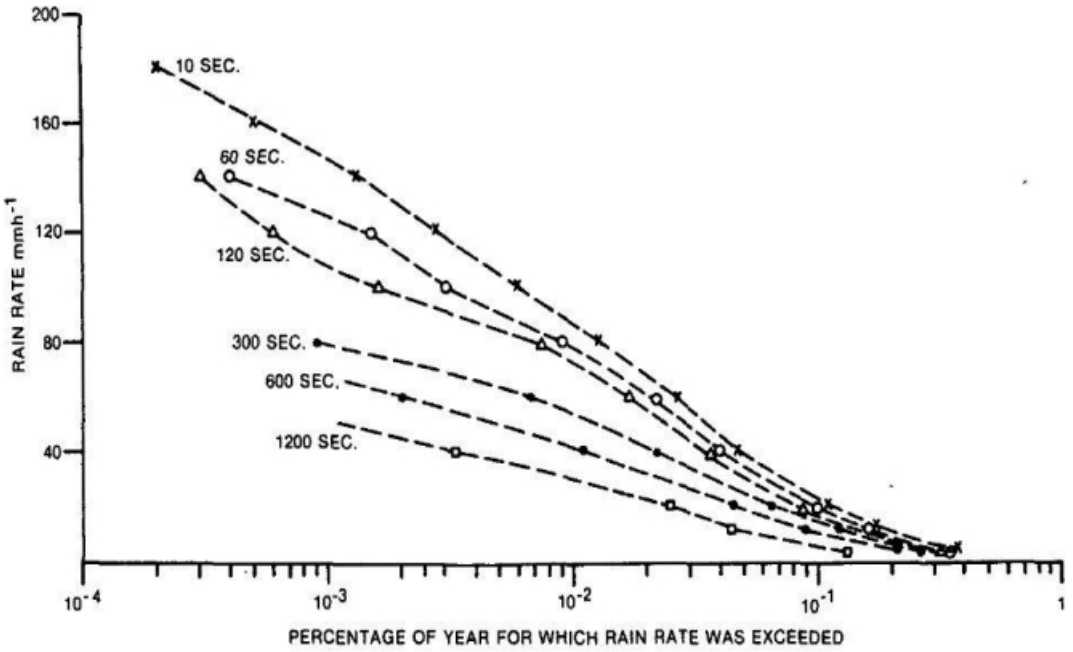

Figure 2.2: loss of data by higher integration time rain gauges [45]

The figure(2.2)shows the rainfall rate CD plots for various integration times, 10sec, 1-min, 2-min, 5-min, 10-min, and 20- min. This has led to researches on methods to be able to infer shorter integration time data from longer available rainfall rate data. Many works have been published that describe various methods of integration time conversion.

1. Segal method

The conversion method is expressed as [46]:

$$R1\left(P\right)=CF\tau\left(P\right)R\tau\left(P\right) \tag{2.1}$$

where conversion factor $CF\tau\left(P\right)=a*P^{b}$, and the parameters a and b denote the regression coefficients

2. Burgueno et al.'s method

Based on 49 years of rainfall data measured at Barcelona, Spain, Burgueno et al used direct power law fit as [47]:

$$R1\left(P\right)=a*\left(R\tau\right)^{b}\left(p\right) \tag{2.2}$$

Where a and b represent the conversion variables obtained from a statistical analysis of rainfall data.

3. Chebil and Rahman's method

Conversion process from 60-min to 1- min integration time as follows [48]

$$CF60\left(P\right)=R1\left(P\right)/R60\left(P\right) \tag{2.3}$$

Where $CF60\left(P\right)$ is expressed as a mixed power exponential law $CF60\left(P\right)=\left(a*P^{b}\right)+c*e^{\left(dP\right)}$ with regression variables represented by a, b, c, and d obtained from a statistical analysis of rainfall data.

4. Logarithmic model

The expression for this model is given as [49]:

$$Log[R1(P)]=alog[R\tau(P)] \tag{2.4}$$

Where a, denotes the regression variable derived from a statistical analysis of the rainfall rate.

5. Exponential model

$$R1\left(p\right)=aexp(b*R\tau\left(p\right)) \tag{2.5}$$

2.4 Specific attenuation

A fundamental quantity that are to calculate the rain attenuation statistics for terrestrial and earth-space paths is the specific attenuation γ or attenuation per unit distance [50]. Two general approaches have

been used to calculate γ by various authors:

- Theoretical method employing a uniform distribution of raindrops modeled as water spheres or more complex shapes
- Empirical method primarily based at the approximate relation among γ and rain rate (R) given as [50]:

$$\gamma = K * R^{\alpha} \tag{2.6}$$

Equation (2.6) is known as the power-law form of rain specific attenuation where R is the rain rate in mm/h K and α are power law parameters These values were adopted by the ITU-R recommendation 838-3 [51].

To discover the values of the power law parameters K and α for both polarization for frequency which lies in among discrete frequencies in [51], logarithmic interpolations are used for f and k, and linear interpolation for α1. s

2.5 Rainfall attenuation predication models

Rain attenuation can be gotten straightforwardly from link estimations or from the information of point rain rate, raindrop size dispersion or other important propagation parameters along the radio way. Propagation tests are done as it were in a number of places around the world and for a restricted number of frequencies, their outcomes cannot be directly connected to all destinations. This can be due to the diverse features and climatic conditions related with each region around the world, which straightforwardly impact the rain in a specific environment. Subsequently, a few attenuation models have been developed based on the physical actualities and accessible propagation information in a specific topographical region. The most center of this chapter is to review the rain attenuation work (experimental and hypothetical) that has been done in different parts of the world.

2.5.1 ITU-R terrestrial rain attenuation model

The ITU-R P.530-17[42] gives a simple technique that may be used for estimating the long-term statistics of rain attenuation. The following simple procedure is presented in this model for estimating the long-term statistics of rain attenuation:

1:- Compute Rain rate $R_{0.01}$ exceeded for 0.01% of the time (with an integration time of 1 min)

2:- Calculate specific attenuation (dB/km) based on Recommendation ITU-R P.838-3[51].

3:- Effective path length(deff)of the link An estimate of this factor is given by:

$$r = 1/0.477 * d^{0.633} * R_{0.01}^{0.073\alpha} f^{0.123} - 10.579\,(1 - exp\,(-0.024d)) \tag{2.7}$$

Where f(GHz) is the frequency and α is the exponent in the specific attenuation model from Step 2.

4:- An estimate of the path attenuation exceeded for 0.01% of the time is given by:

$$A = \gamma\,(R) * d_{eff} = \gamma\,(R) * d_r \tag{2.8}$$

5:- The attenuation exceeded for other percentages of time p in the range 0.001% to 1% may be deduced from the following power law:

$$A_P/A_{0.001} = C_1 * P^{-(C_2 + C_3 Log_{10} P)} \tag{2.9}$$

$$C_1 = \left(0.007^{C_0}\right)\left[0.12^{1-C_0}\right] \tag{2.10}$$

$$C_2 = 0.855C_0 + 0.546\,(1 - C_0) \tag{2.11}$$

$$C_3 = 0.139C_0 + 0.043\,(1 - C_0) \tag{2.12}$$

$$C_0 = \begin{Bmatrix} 0.12 + 0.4\left[Log_{10}(f/10)^{0.8}\right], f \leq 10GHz \\ 0.12, f < 10GHz \end{Bmatrix} \tag{2.13}$$

6:-Calculate the annual time percentages p corresponding to the worst-month time percentages using climate information specified in Recommendation ITU-R P.841-5[52].

2.5.2 Crane attenuation models

There are three versions of the Crane demonstrate. The Worldwide Crane demonstrate ,two-component model, last version of the two-component model. This points to progress the spatial relationship suspicions and the measurable changes of precipitation in cell [37].

- Crane Global Rain Attenuation Model

Crane Worldwide show [37] was created for earthly paths. This show is totally based on geophysical perceptions of vertical changes in precipitation, precipitation structure, and temperature. The resulting attenuation demonstrate for a given rain rate is given by:

$$A_T = \gamma(R)\left(exp\left(y\delta(R)\right)/y\right) * exp(zD) - exp\left(z\delta(R)\right)/y * exp(\alpha\beta), \delta(R) < D < 22.5 \tag{2.14}$$

$$A_T(R, D) = \gamma(R)\left(exp\left(\gamma y\delta(R)\right)/y\right), 0 < D < \delta(R) \tag{2.15}$$

Where A_T is the horizontal path attenuation (dB), R the rain rate (mm/h), D the path length (km) and $\gamma(R)$ the specific attenuation.

$$B = ln(b) = 0.83 - 0.17ln(R) \tag{2.16}$$

$$C = 0.26 - 0.03ln(R) \tag{2.17}$$

$$\delta(R) = 3.8 - 0.6ln(R) \tag{2.18}$$

$$U = B/\delta(R) + C \tag{2.19}$$

$$y = \delta(U) \tag{2.20}$$

$$z = \delta(c) \tag{2.21}$$

2.5.3 Moupfouma's model

The rain attenuation is defined as [38]:

$$A_{0.01} = KR_{0.01}^{\alpha} L_{eq}(R_{0.01}, L) \tag{2.22}$$

Where $R_{0.01}$ and $A_{0.01}$ are the rainfall rate and path attenuation at 0.01% of time. Leq is the propagation path length given as:

$$L_{eq}(R_{0.01}, L) = L * exp\left(-R_{0.01}/1 + \zeta(L) R_{0.01}\right) \tag{2.23}$$

Additionally, this model gives a method to determine the occurrence of attenuation due to rain on a given microwave link as:

$$P(A_{0.01}) \geq \alpha = 0.01\left(A_{0.01/\alpha+1}\right)\phi(\alpha)\, exp\left(9.21\left(1 - (\alpha/A_{0.01})\right)\eta(\alpha)\right) \tag{2.24}$$

$$\phi(\alpha) = (\alpha/A_{0.01})\, ln(\alpha/A_{0.01} + 1) \tag{2.25}$$

2.6 Spatial Interpolation Techniques for Rainfall Data

Rainfall distribution plays a vital role in understanding the hydrological process. In order to run hydrological modeling, spatial interpolation of rainfall data is a key parameter. Geographic Information System (ArcGIS) is used to estimate the spatial distribution. The accuracy analysis is implemented using Cross Validation (CV) on the interpolated rainfall, surface. Validation made use of rainfall stations to pick the most suitable interpolation method which gives an enhanced accuracy.

2.6.1 Spatial interpolation methods for calculating rainfall

Spatial interpolation methods can be divided into two main categories:
1. Deterministic approaches
2. Geo-statistical approaches
To put it easy, deterministic approaches do not attempt to capture the spatial structure in the data.The solely build use of pre-defined mathematical equations to predict values at unsampled locations. On the contrary, Geo-statistical approaches intend to fit a spatial model to the data. This allows to generate a prediction value at unsampled locations (deterministic methods) and to give users with an estimate of the accuracy of this prediction. Deterministic methods are TIN, IDW and Trend surface analysis techniques. Geo-statistical approaches include kriging and its variants. Interpolation techniques depend on the actual fact that spatial datasets exhibit some spatial correlation. Interpolation methods may used to predict values at specific locations within the field or over an entire grid of interpolation. during this case, this grid is created of regularly spaced pixels whose size can rely on the specified accuracy of the interpolated map or on the spatial structure of the data set.

Deterministic interpolation methods

Regarding the primary group of spatial interpolation methods for measuring rainfall, the foremost frequently used deterministic methods are Inverse Distance Weighting (IDW), which are depend on measured values. Generally, the forecast of the regionalized value takes under consideration the weighted average of the observed regionalized values.

- **IDW (Inverse Distance Weighting)**

Inverse Distance Weighted interpolation explicitly implements the opinion that things that are near each other are more alike than those that are farther apart [53].To expect a well worth for any unmeasured region, IDW will use the measured values surrounding the expected region. The ones measured values closest to the prediction location may have more affect at the anticipated value than the ones farther away. Thus, IDW assumes that every measured point contains a local influence that diminishes with distance. The predictor of IDW is created as a weighted sum of the data.

Geostatistical interpolation methods

The second group of spatial interpolation techniques used to measure rainfall, geostatistics techniques, constitute a discipline that connects mathematics and earth sciences. Kriging is an example of a set of geostatistical techniques used to interpolate random field values. Kriging is based on a statistical model that involves autocorrelation. The autocorrelation is transformed into a statistical correlation between the measurement points. Geostatistical methods not only have the ability to generate prediction surfaces, but also provide some measures of certainty and precision of predictions.

- **Kriging**

Krige (1951) and Matheron (1963) developed the Kriging method. Its name is derived from the Kriging method and is used to predict or reserve reserves based on samples collected in mining areas [54]. Kriging is the most widely used geostatistical method in spatial interpolation. The Kriging technique is based on the spatial model (defined by the variogram) between observations to predict the values of the attributes of the locations without sampling. One of the peculiarities of the kriging methods is that they not only consider the distance between observations, but also aim to capture the spatial structure of the data by comparing two observations separated by a specific spatial distance at the same time. The purpose is to understand the relationship between observations separated by different delay distances. All this knowledge is contained in the variogram. Then, the Kriging method derives the spatial weight of the observations based on the variogram. Note that the kriging technique retains the initial sample values in the interpolation graph. Kriging is a powerful type of spatial interpolation, which uses complex mathematical formulas to estimate the value of the unknown point based on the value of the known point. There are several different kriging methods: ordinary kriging, general kriging, co-kriging, and instruction kriging [55]. For this paper, the most common type, ordinary kriging, was selected.

kriging formula

Kriging is similar to IDW in that it weights the surrounding measured values to derive a prediction for an unmeasured location. The general formula for both interpolation is formed as a weighted sum of the data:

$$Z(s_o) = \sum_{i=1}^{N} \lambda_i z(s_i) \tag{2.26}$$

where:

$z(s_i)$ = the measured value at the ith location

λ_i = an unknown weight for the measured value at the ith location

s_o = the prediction location

N = the number of measured values

Creating a prediction surface map with kriging

To use Kriging interpolation to make predictions, you need to complete two tasks[56]:

- Reveal correlation rules
- Make predictions

To accomplish these two tasks, Kriging goes through a two-step process:

- Creates a variogram and a covariance function to estimate the statistical correlation(called spatial auto correlation). The value depends on the autocorrelation model(Compatible with model).
- Predict unknown values(makes pridiction).

Because of these two different tasks, some people say that Kriging uses data twice: the first time is used to estimate the spatial auto correlation of the data and the second time is used for prediction.

Variography

Fitting a model, or spatial modeling, is also known as structural analysis, or variography. In spatial modeling of the arrangement of the measured points, start with a graph of the empirical semivariogram, figured out with the following equation for all pairs of locations divided by distance h:

$$Semivariogram(distance_h) = 0.5 * avarage((value_i - value_j)^2) \tag{2.27}$$

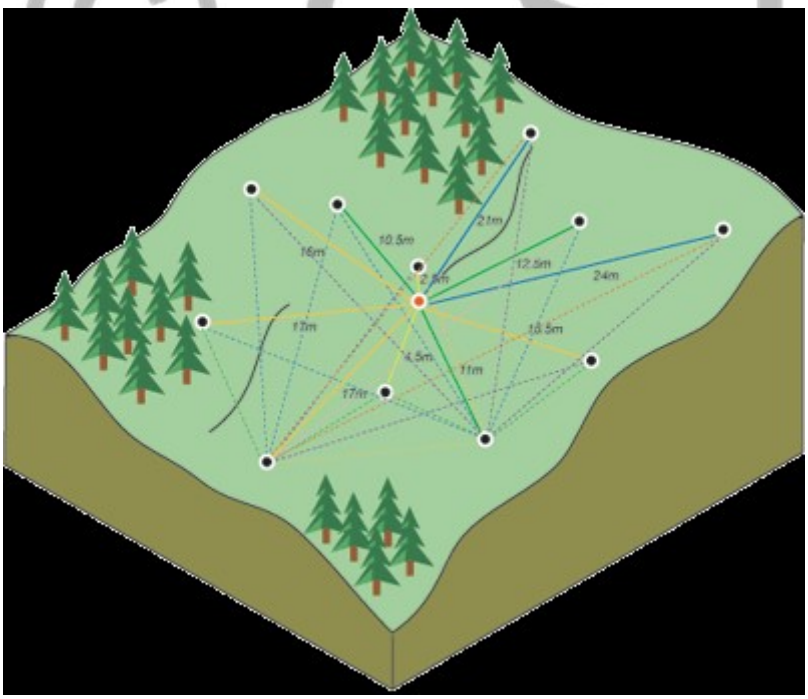

Figure 2.3: Calculate difference squared between the paired locations [57]

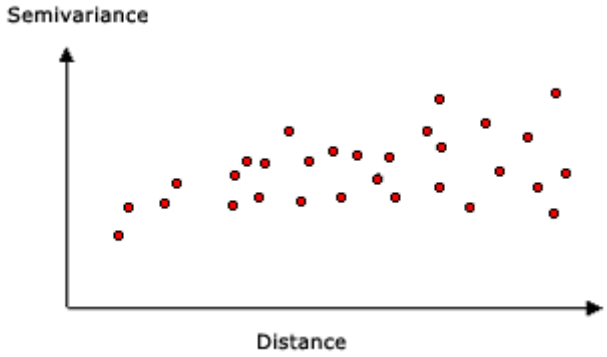

Figure 2.4: Empirical semivariogram graph [57]

Spatial autocorrelation specifies a key principle of geography: things that are closer are more alike than things distantly apart. Therefore, pairs of locations that are closer (far left on the x-axis of the semivariogram cloud) should have better similar values (low on the y-axis of the semivariogram cloud). As pairs of locations become farther apart (moving to the right on the x-axis of the semivariogram cloud), it should become more dissimilar and have a higher squared difference (going up on the y-axis of the semivariogram cloud).

Fitting a model to the empirical semivariogram

Semivariogram modeling is a guided step between spatial description and spatial prediction. The main application of kriging is the prediction of attribute values at unsampled points. The empirical semivariogram provides information on the spatial autocorrelation of datasets. However, it does not provide information for all available directions and distances. For this reason, and to ensure that kriging predictions have the positive kriging variant, it is crucial to fit a model that is, a continuous function or curve to the empirical semivariogram. Abstractly, this is similar to regression analysis, in which a continuous line or curve is fitted to the data points.

However, if it add the distance each point is above the line and add the distance each point is below the line, the two values should be identical. There are many semivariogram models from which to choose[56].

Semivariogram models

The Kriging tool provides the following functions from which to choose for modeling the empirical semivariogram:

- Circular
- Spherical
- Exponential
- Gaussian
- Linear

The selected model influences the prediction of the unknown values, particularly when the shape of the curve near the origin differs significantly. The steeper the curve near the origin, the more influence the closest neighbors will have on the prediction. As a result, the output surface will be less smooth. Each model is designed to fit different types of phenomena more accurately.

The diagrams below show two common models and identify how the functions differ:

A spherical model example

This model shows a progressive decrease of spatial autocorrelation (equivalently, an increase of semivariance) until some distance, beyond which autocorrelation is zero. The spherical model is one of the most commonly used models.

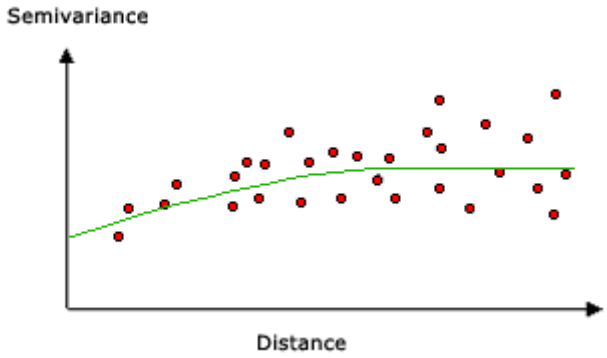

Figure 2.5: Spherical model [56]

An exponential model example

This model is applied when spatial autocorrelation decreases exponentially with increasing distance. Here, the autocorrelation disappears completely only at an infinite distance. The exponential model is also a commonly used model. the selection of which version to apply is primarily based on the spatial the selection of which version to apply is primarily based on the spatial autocorrelation of the statistics and on earlier information of the phenomenon. autocorrelation of the statistics and on earlier information of the phenomenon.

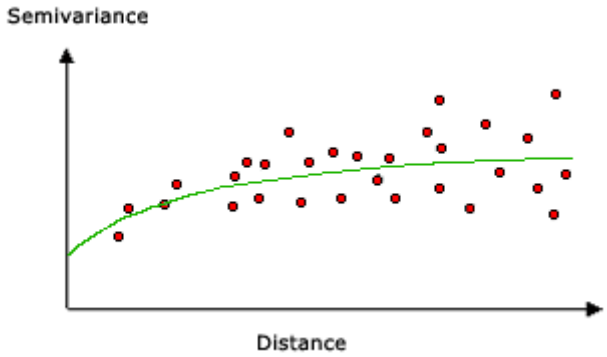

Figure 2.6: Exponential model [56]

2.6.2 Accuracy assessment interpolation methods

In this section, a way of various prediction accuracy assessments of assorted interpolation techniques discussed. There are two common validation methods that are widely suggested for evaluating the accuracy of interpolation methods. the primary method could be a cross-validation method, namely as a leave-one-out technique. the other validation method is named the split sample method.

1. Cross-validation method

Cross-validation could be a statistical technique of evaluating and comparing the performance of various interpolation methods [55][53]. This method involves omitting one sample value from the whole dataset and performing an interpolation procedure by using the remaining dataset. After the interpolation process, the difference between the particular and predicted values of the omitted point is then calculated. This procedure is repeated for n times, where n equal to the amount of all samples.

2. Split-Sample method

In this method, the complete raw dataset is split into two subsets: the training dataset and therefore the test datasets. The training dataset is to produce the interpolated surface, and therefore the performance of every interpolation method is evaluated by comparing the difference between the expected and observed values from the test dataset.

Several statistical measurements are most generally used to evaluate the overall performance of interpolation methods. The accuracy evaluation indices commonly used include,(ME),(MAE),(MSE) and (RMSE) For n observations, p predicted value, and o observed value these indices are evaluated using the expressions listed below [58]:

$$ME = 1/n \sum_{i=1}^{n} (p_i - o_i) \tag{2.28}$$

$$MSE = 1/n \sum_{i=1}^{n} (p_i - o_i)^2 \tag{2.29}$$

$$RMSE = \left[1/n \sum_{i=1}^{n} (p_i - o_i)^2 \right]^{1/2} \tag{2.30}$$

Cross-validation is used along with these measurements to assess the performance of the interpolation methods. during this paper the ME and RMSE (available on the software used) are used to evaluate the performances of the IDW and Kriging interpolation methods considered within the analysis part of this work.

Chapter 3

Rainfall Data Measurement, Processing and modeling

3.1 Introduction

In this section, the step-by-step detailed approach used to assess the effect of rain on terrestrial line of site paths in the micro and millimetric frequency bands is presented. The rainfall data measurement processing and modeling section of the thesis is organized as follows: Section 3.2 discusses climatic characteristics of Ethiopia; Section 3.3 focuses on the rain measurement and data processing; Section 3.4 focuses on modeling of one-minute rainfall rate cumulative distribution; Section 3.5 discussed on the determination of rain attenuation over Ethiopia and finally, Section 3.6 gives an insight into the prediction of rain attenuation model for Ethiopia from live measurements.

3.2 Geography and Climate of Ethiopia

Geographically, Ethiopia is located in the Horn of Africa between latitudes 30^o N to 180^o N,longitude 33^oE to 48^o E , with an altitude variation from 100 meters below sea level to over 4000 meters above sea level. It is bordered by Eritrea to the north, Djibouti and Somalia to the east, Sudan and South Sudan to the west, and Kenya to the south, as shown in Figure 3-1. Ethiopia is generally a country of plateaus, with the Great Rift Valley separating the western and eastern highlands. The highlands slowly slope to the lowlands of Sudan to the west and Somalia to the east [17].

Figure 3.1: Maps of Ethiopia[17]

3.3 Rain Measurement and Data Processing

The reliability of wireless networks operating at microwave and millimetre-wave bands is often constrained by the intensity of rainfall for a particular locality. It is therefore usual for radio engineers to include the contribution of rainfall attenuation to overall link budget to guarantee satisfactory performance of radio links all year round. To achieve this, the point rain rate R0.01 (in mm/h), i.e. rainfall rate exceeded for 0.01% of an average year, is determined from rain rate measurements of one-minute integration time. Not unusually, rainfall measurements at one- minute integration time are often scarce to obtain in Africa, and by extension, in Ethiopia. However, many meteorological agencies across different African countries regularly archive rainfall data of longer integration time often hourly and daily measurements, which are obtained from networks of rain gauges. In the absence of appropriate one-minute rainfall data, there exist some other valid rain rate climatological models to convert rainfall data from higher integration time to lower integration time. These rain rate models may suffice as alternatives for evaluating rainfall parameters for designing wireless communication systems operating at microwave and millimetre wave bands.

3.3.1 Rain measurements and data processing

Agreeing to the suggestion of ITU-R rain attenuation forecast procedures[42], the foremost successful way of deciding total precipitation dispersion is through coordinate estimation made at the location of interest.To facilitate the application of the proposed rain rate distribution models, a reliable source of long-term rainfall measurements is required for different sites in Ethiopia. For this purpose, different devices are available to record rainfall. The NMA of Ethiopia uses two techniques to collect rain data,

namely, it applies networks of rain gauges to measure rainfall intensity every 24 hours, and automated rain gauges to record rainfall intensity per 15 minute. The gauges meet the World Meteorological Organization standards. For the purpose of this section , (7-10 years) Raw rainfall data collected by NMA (Automated rain gauges to record rainfall intensity per 15 minute) comprising rainy and non-rainy (zero value) days is considered. Only the rain intensities with values different from zero were sorted out and prepared, and after that the suitable numerical formulation was utilized to calculate the desired parameters.

3.3.2 15- Minute rainfall rate distribution in Ethiopia

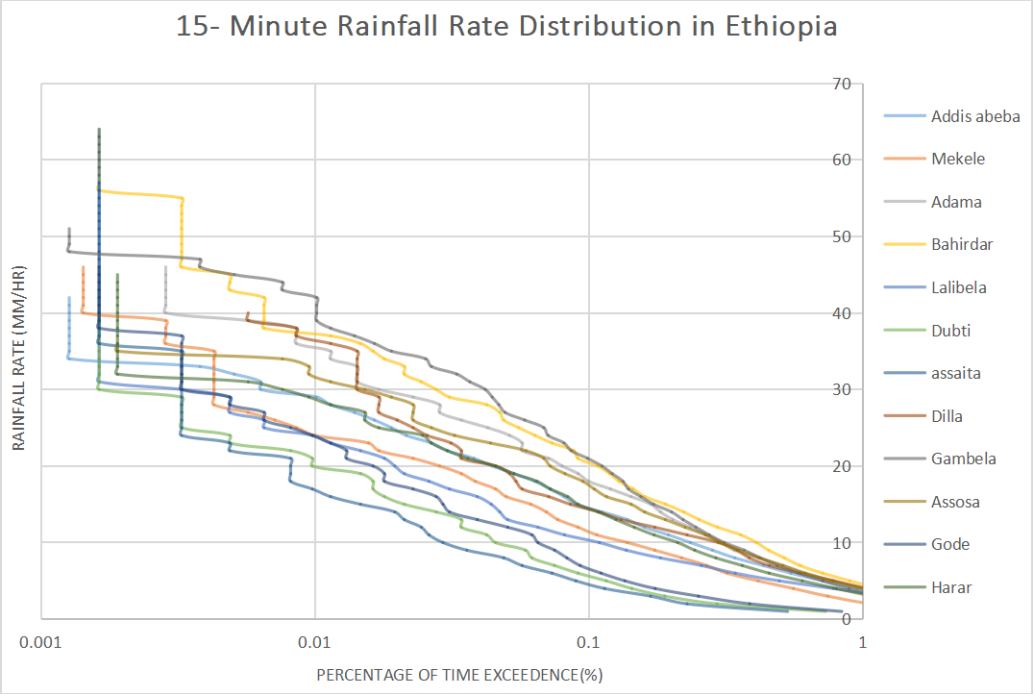

Figure 3.2: Distribution at 15-minute sampling rate in Ethiopia

Table 3.1: 15min (mm/h) for 99%, 99.9%, and 99.99% availability

Location	M (mm/hr)	0.10%	0.01%	0.00%
Addis Ababa	975.6	15.87	27.56	39.26
Lalibela	755.6	9.02	22.24	54.84
Bahir Dar	1213.4	21.79	40.66	59.53
Asaita	119	4.3	16.74	65.13
Dubti	150.6	5.57	16.87	51.07
Assosa	1045.8	17.7	30.28	42.86
Gambela	996.9	21.26	38.33	55.4
Harar	786	15.67	28.63	41.59
Adama	981.5	19.08	34.45	49.83
Gode	193.8	6.44	20.27	63.79
Dilla	1038.3	17.77	32.16	49.55
Mekele	521.8	13.3	27.57	41.83

Figure 3.2 shows rain rate distribution for different main sites of Ethiopia versus percentage of exceedance for the 15-minute precipitation rate. Procedure for cumulative rainfall rate distribution

- Calculate frequency from the range of rain rate
- Calculate probability from frequency
- Calculate PDF and CDF
- Calculate CCDF
- Calculate percentage of exceedance and plot the cumulative distribution

3.4 Modeling of One-minute Rainfall Rate

3.4.1 Rain rate integration time conversion

The integration time conversion of rain rate is an important step for any propagation study in related to rain. It is a means of extracting shorter integration time rain rate values (with higher intensity) from longer integration equivalent time series rain rate records (lesser intensity). Conversion methods reviewed in chapter two section(2.3).

3.4.2 Determination of R0.01

Ensuring 99.99% system availability the design of microwave and millimeter wave links requires knowledge about the worst-case attenuation levels. For attenuation levels related to rain, this is possible by considering the rain rate exceeded for 0.01% of the time in a year, commonly known as R0.01. R0.01 should be of 1-min integration time using different conversion models as described in chapter 2.The accuracy of conversion model is compared against measurement results in the section(4) As a result, on this studies work, used one- minute rainfall rate recorded with a tool mounted at Jimma university, Ethiopia which includes rainy and non-rainy (zero value) days is applied. Most effective the rain intensities with values different from zero had been sorted out and processed, after which the suitable mathematical method became used to calculate the preferred parameters. Therefore, the study have got locally measured rain rate data with 1- minute integration time. Given one has the raw rate intensity data, this a very quick and simple method of arriving at R0.01%. The procedure is briefly outlined

- Filter rain rate raw data and remove recordings with blank reading. Different measuring device have different means of communicating times when there was no recording for some reason, so the particular equipment is setting and syntax should be followed.
- Sort the rain rates in an ascending order
- Assign cardinal numbers n for the rain rate values like n = 1,2, 3. . . , Nr
- Determine the number of non-zero recordings, Nr.
- Calculate the percentage for each r>0mm/h recording by the following formula
- Read the rain rate value along p(%)=0.01 , which is the value of R0.01%

$$P(\%) = N_r - n/Numberofminutsinayear * 100 \tag{3.1}$$

3.4.3 Contour mapping of rainfall rate distribution for Ethiopia

For the development of rain rate contour maps at different time of exceedance at 0.1% and 0.01%, data set obtained from conversion factors. Therefore, by applying procedures of conversion model, one-minute rain rate contour maps for Ethiopia are developed. Contour map for rain rate exceedence at 0.1% and 0.01% were developed using a Geographic Information System (GIS) software platform, the ArcGIS®. Contour results from this Contour outcomes from this software program had been sequenced by applying in-built gridding approach through the Kriging interpolation technique, and, therefore mapping the generated contour outputs into focused coordinate points on the digital map of Ethiopia.

3.5 Determination of Rain Attenuation over Ethiopia

3.5.1 Determination of specific rain attenuation of rainfall

Determine the specific rain attenuation (dB/km) for 12 geographical locations in Ethiopia at horizontal and vertical polarization have been computed based totally on the worldwide ITU-R model. The use of the real local rain rate information from those places, the rain rate R0.01 exceeded for 0.01% of the time turned into decided from the cumulative distributions in their rainfall-rate for an integration time one-minute. this is determined for averaged over the duration of (7-10) years. Further, the ITU-R average rain rate R0.01 values passed for 0.01% of the time with one-minute integration time of the average yr for Ethiopia have been utilized to compute the particular attenuation for those places.

3.5.2 Specific attenuation contour mapping for Ethiopia at 11 GHz and 27 GHz

As the efforts to make certain minimal interference of wireless community provider by means of rainfall activities, radio hyperlinks layout need to correctly deal with signal deterioration at microwave and millimetre bands, mainly in tropical and equatorial areas in which Ethiopia is placed. Therefore, it is imperative to develop contour maps from ITU recommendations at 99.99% link availability, for terrestrial link deployments across Ethiopia.

In line with this, particular attenuation was at first computed for different locations at rain rate exceedence of 0.01% of time. Thereafter, results from these computations were exported to ArcGIS® software to generate contour maps which demonstrate the spatial variation of specific attenuation over Ethiopia. To this end, rainfall specific attenuation contour maps have been produced for the entire country for the design of future radio links operating at carrier frequencies of (11 GHz) and (27 GHz). These bands are tremendously liable to rain attenuation impact, but they present awesome possibilities in the destiny for community operators, due to their channel potential for large service bandwidths required to satisfy the developing traffic call for of wireless offerings .

3.5.3 Determination of path attenuation over Ethiopia

These three models had been defined based on the accessible nearby propagation information and have been extended to other parts of the world. The hypotheses and the directing equations for all these three models were definitely expressed and appeared in Chapter Two (section 2.8) of this work

- The ITU-R long-term statistics of rain attenuation model
- The Moupfouma model
- The Global Crane model

3.6 Prediction of Rain Attenuation Model for Ethiopia from Measurements

At this step that have utilized to compare existing rain prediction methods with received signal level estimations for the earthly LOS interface in between Addis Ababa(9.01^{o}N, 38.44^{o}E) and Furi(8.5258^{o}N, 38.41^{o}E) is attempted in collaboration with Ethiotelecom at 11 GHz and 16.42 km, estimations were taken with vertical polarization for the year 2015 that recorded between the two radio transmitting paths.

Chapter 4

Result and discussion

4.1 Introduction

This chapter of the thesis where the findings of the research study are discussed. Because the thesis part involved not only analyze suitable rain attenuation prediction models and developing contour maps, but also all the factors contributing to the final formulations. Detailed discussion of the following topic is presented; determination of rain rate exceedance values, specific rain attenuation (dB/km) for different geographies Locations are computed based on the available rain rate data ,frequency and polarization and develop contour map at 11 and 27 GHz frequency with vertical and horizontal polarization. Moreover the path attenuation (dB) for areas is in this way estimated by using the existing models of the accessible local rain information. From there, a suitable rain attenuation model is proposed for Ethiopia. The rest of this chapter presents these issues in the order set out above.

4.2 Rain rate integration time conversion

Before discussing the conversion of the integration time, the cumulative rainfall distribution for Jimma was made according to the available measured data. This can be seen in Figure(4.1). This distribution serves as a point of reference for developing the conversion technique.

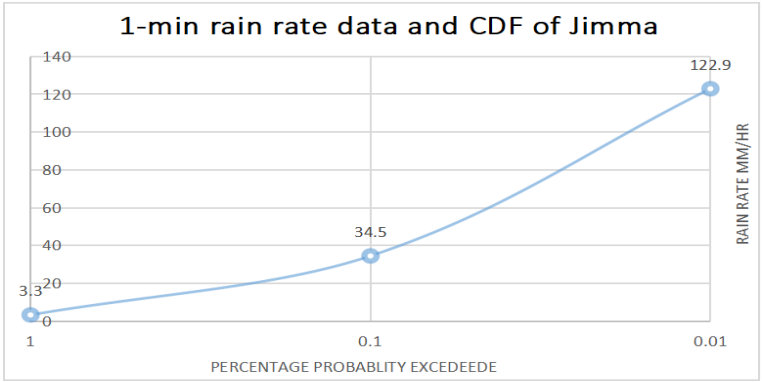

Figure 4.1: 1-min rain rate data and CDF for Jimma. R0.01%=122.9mm/h.

The first method of conversion used to convert the integration time was the equation of the power law defined in Chapter 2. The starting point for any conversion calculation is the Jimma 1-min rain rate distribution. Coefficients and were determined and these were used for other locations since only 15-min integration time for the other locations were available for this research work. The result of curve fitting is presented in Figure (4.2). The correlation coefficient is also shown on the figure. A value of 0.98 can be improved using other methods. Research has shown that a correlation coefficient greater than the above value is achieved using the conversion factor approach.

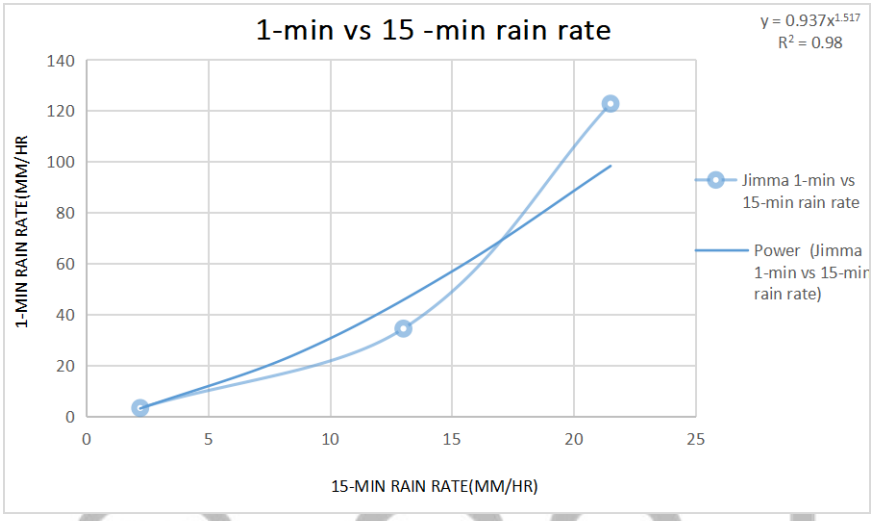

Figure 4.2: Power law curve fitting, 1-min Vs 15-min in measured rain rate (Jimma)

Because of the lack of 1 min measured data for other locations in Ethiopia, the research used the result of converting the integration time for the Jimma site to other cities as well. The research work showed the results of the two approaches, i.e., the power law and the conversion factor methods, are presented. Due to the similarity in the rain process across these locations the work reasoned that the method doing well for Jimma site could as well give a better estimation result than other estimation methods.

The 1-min probability exceedance levels were fitted against the 15-min data (both are measured set of rain rate data) for Jimma city to find the conversion coefficients and for power law method defined by:

$$R(P)_1 = CF * R(P)_{15} \tag{4.1}$$

Where,$CF = aP^b$ First, the conversion factor CF is fitted against the probability levels as shown in Figure (4.3) The second method clearly shows better estimation ability than the first one. As it is shown in Figure (4.3) , The correlation coefficient , 0.9928 is also close to unity, clearly indicating how close the measured and fitted data are.

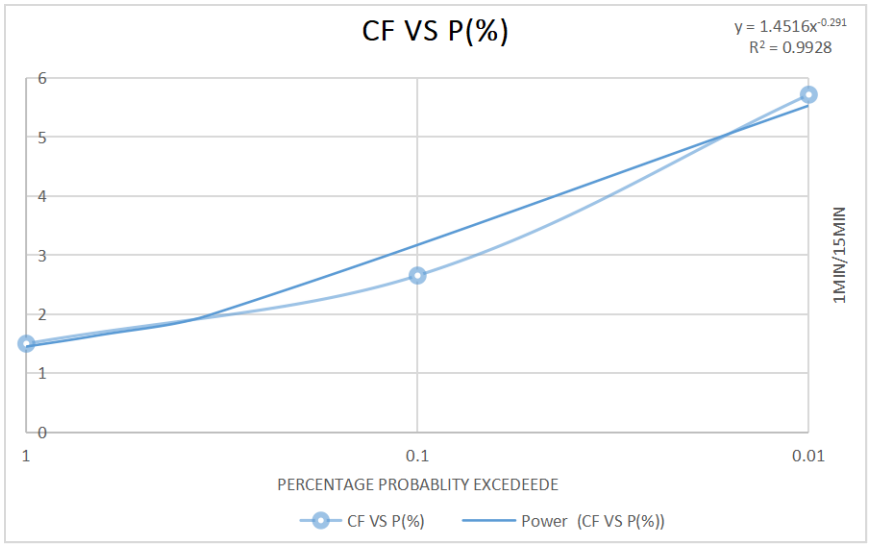

Figure 4.3: $CF = aP^b$ for 0.001<p<1(a=1.451607, b= -0.29051)

This CF values are then used to calculate the estimated 1-min rain rate values as $R(P)_1 = CF * R(P)_{15}$.$R15$.

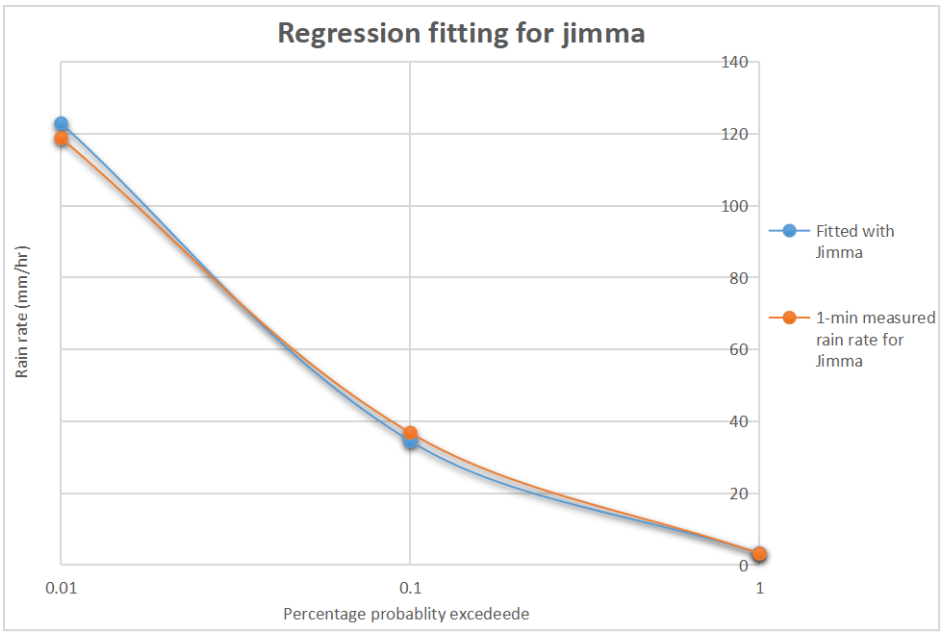

Figure 4.4: Regression fitting for jimma ,integration time conversion with $CF = aP^b$

Table 4.1: Percentage errors of estimation of New conversion methods and ITU

Site -name	Jimma	New conversion methods		ITU	
%p	m(t=1)	e(t=1)	%error	e(t=1)	%error
0.01	122.9	118.8	-11879	84.76	-8475
0.1	34.5	36.82	-367.2	29.26	-291.6
1	3.3	3.19	-2.19	5.89	-4.89

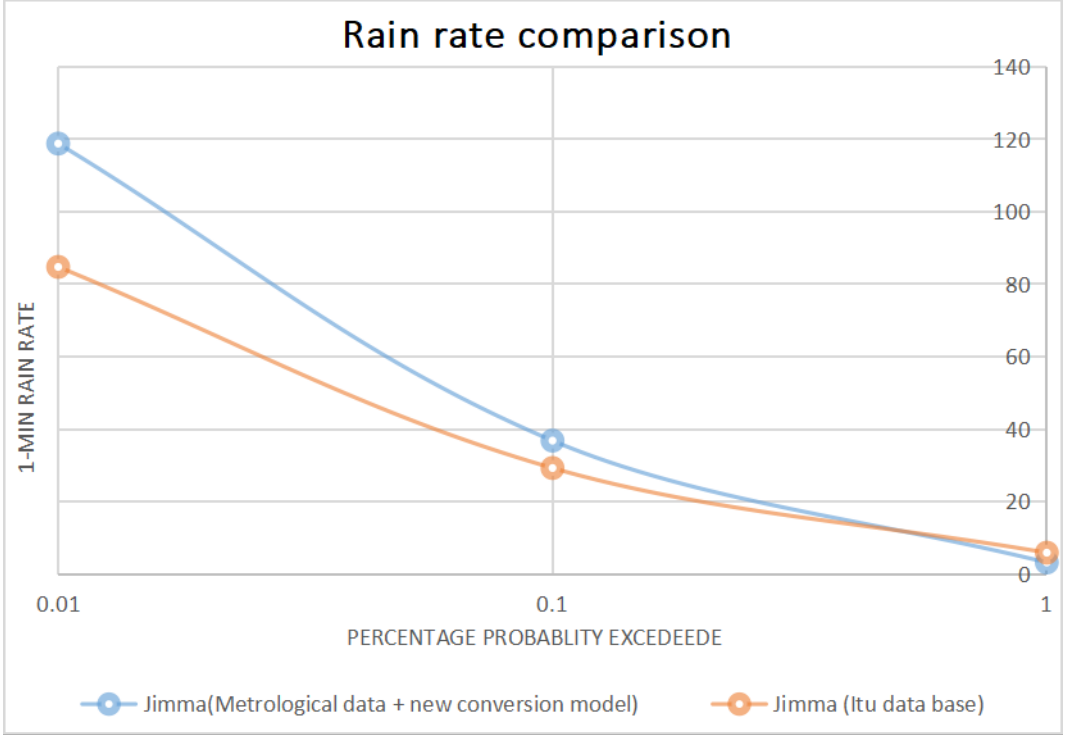

Figure 4.5: Rain rate comparison

From Figure 4.5 shows that the reliable long-term local rainfall rate data for Jimma with 1-min integration times which is different rain rate sample with ITU 837-7 pridicted and underestimated due to temperate climate rain data. So ,it is better to used new conversion model(conversion factor method) for other location with in Ethiopia. Their similarity in rainfall formation and orographical process between places on Ethiopian territory. Integration time conversion coefficients based on Jimma rainfall data should provide better estimation results than ITU models based on temperate climate rainfall data. The estimated 1-min rain rate values for few selected cities is given below in Table (4.2)

Table 4.2: Conversion factor R0.01% estimate based on Jimma (m=measured, e=estimated)

p(%)	Jimma		AA	Mekele	Bahirdar	Lalibela	Dubti
0.01	122.9	21.5	118.88	152.8	152.84	225.44	123.3	93.54
0.1	34.5	13	36.823	45.01	37.74	61.82	25.58	15.81

4.3 Cumulative Distribution of Rain Intensities for Different Geographical Locations

Cumulative distributions (CD's) of maximum 10 years 1-minute rain intensities for the 12 geographical locations in Ethiopia are plotted in Figure 4.6.

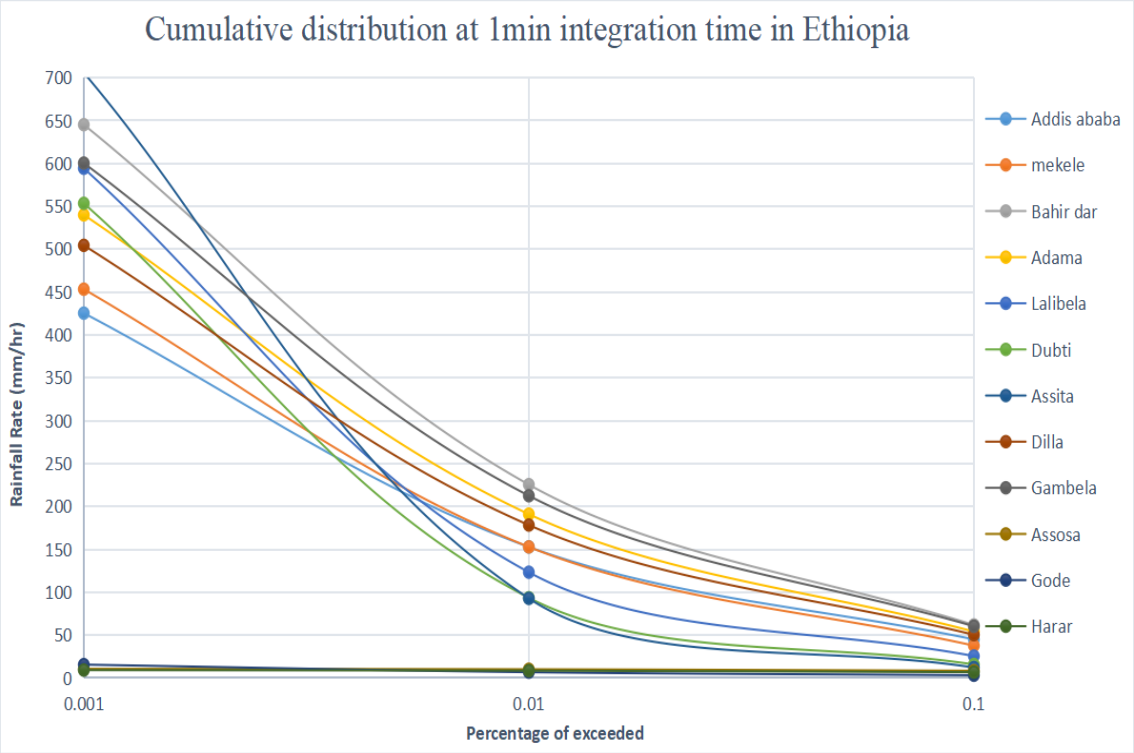

Figure 4.6: Cumulative distribution of rainfall rate using new conversion factor model

From the figure 4.6,it can be seen that the maximum rain rate (R) at 0.001%, 0.01%, and 0.1% of exceedance of time is in Bahirdar,at the same time as the minimum is recorded in Gode.Therefor, it may additionally be located here that Bahirdar have higher rain rates than the alternative regions of Ethiopia and greater susceptible to rain attenuation.

4.4 Rain rate contour mapping over Ethiopia

Contour results from ArcGIS software were sequenced by applying inbuilt gridding technique via the Kriging interpolation method, and, consequently mapping the generated contour outputs into targeted coordinate points on the digital map of Ethiopia.

A quick look at Figure 4.7(a) shows that R0.1 varies from 9.18 to 43.16 mm/h, while in Figure 4.7(b); R0.01 varies from 27.39 to 157.9 mm/h, depending on the location. It is observed that locations lying around the Northern and Southern-West parts of Ethiopia have the highest rainfall rates at both 0.1% and 0.01% rain rate exceedences. With the exception of some locations in the Eastern with lower rain rate exceedences, R0.1 and R0.01 can be approximated to 10 mm/h and 30 mm/h respectively as seen from contour maps.

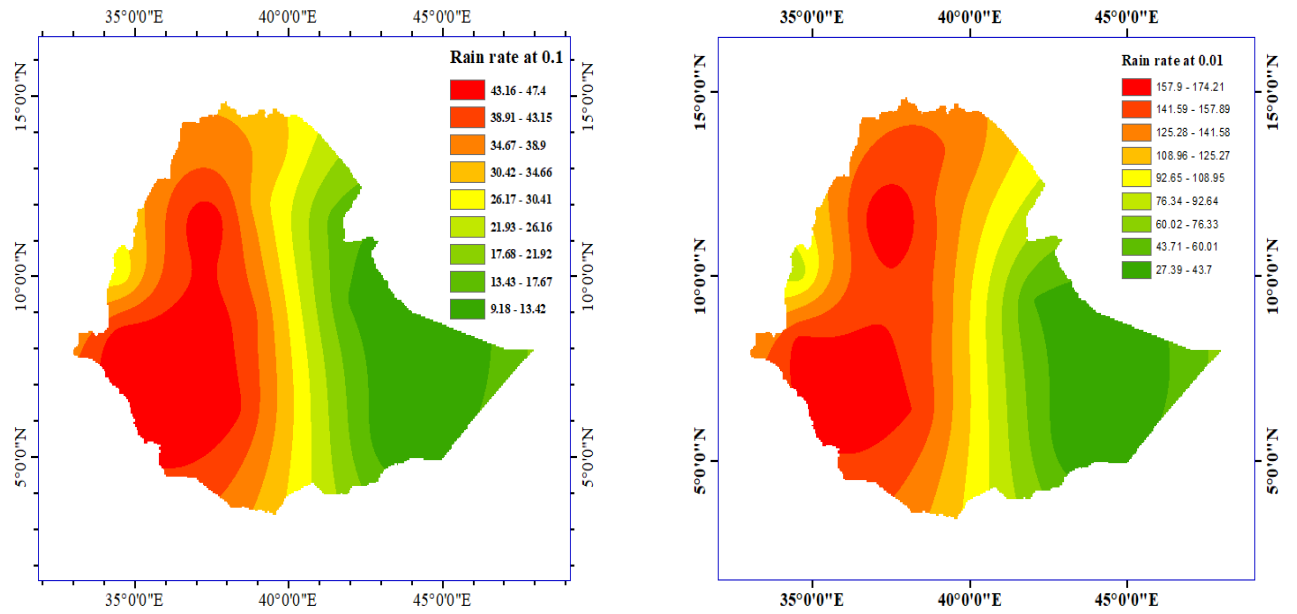

(a) Rainfall Rate(mm/h)for 0.1% of time in Ethiopia (b) Rainfall Rate(mm/h)for 0.01% of time in Ethiopia

Figure 4.7: Rainfall Rate(mm/h)for different exceedence of time in Ethiopia

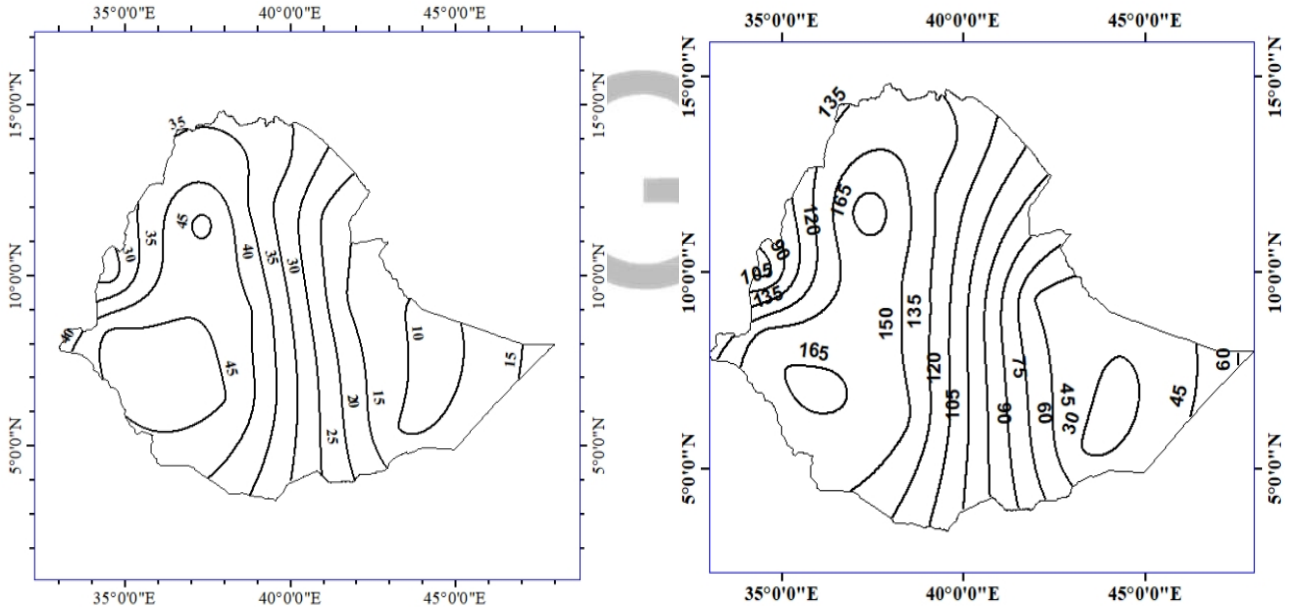

(a) Rainfall Rate (mm/h) contour maps for 0.1% of time in Ethiopia

(b) Rainfall Rate (mm/h) contour maps for 0.01% of time in Ethiopia

Figure 4.8: Rainfall contour map for different exceedence of time in Ethiopia

It is also observed that at stations with close proximity to central Ethiopia close to Addis Ababa, R0.1 and R0.01 may be roughly approximated to 45 mm/h and 145 mm/h respectively.

Table 4.3: The rain parameters required by Ethio-Telecom

Vendors	ZTE	Huawai	Erricson
Rain Method	ITU-R P.530-8	ITU-R P.530-8	ITU-R P.530-8
Rainfall rate	ITU-R P.837-5	ITU-R P.837-5	ITU-R P.837-5
Specific attenuation model	ITU-R P.838-3	ITU-R P.838-3	ITU-R P.838-3
Rain Region	Rain zone map E (J)	ITU-R database	E(rain zone maps)
Reliability Method	ITU-R P.530-12	ITU-R P.530-12	ITU-R P.530-12

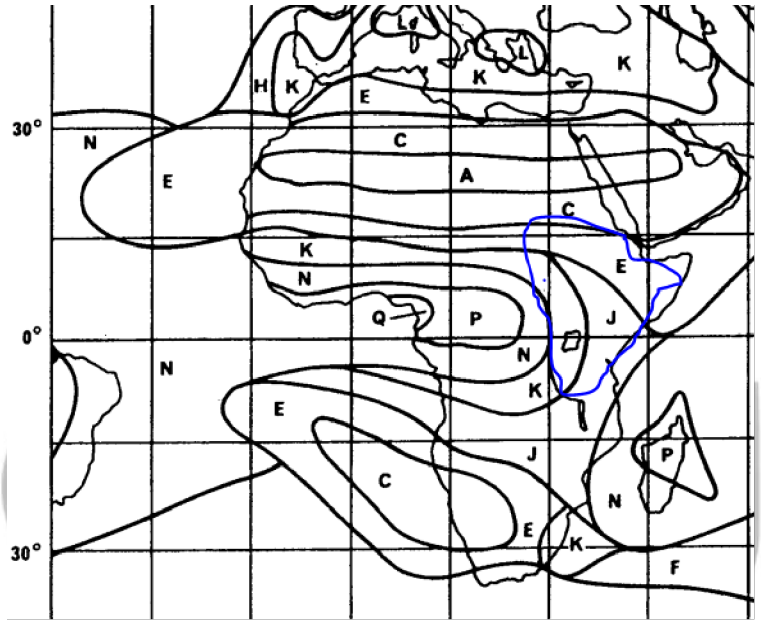

Figure 4.9: ITU-R classifications for Ethiopia

Table 4.4: The rain parameters required by Ethio-Telecom compared with new result

	Vendors results		New result
	ZTE/ERRICSON	HUAWAI	New conversion model
Rain rate(mm/hr)at 99.99%	Contour map(E)	Data base	Contour map and database
Site(Jimma)	22 mm/hr	84.76 mm/hr	118.88 mm/hr

Using ITU-R P 837-6 suggestion[41], Ethiopia has four precipitation climate zones particularly, C, D, E, and J. In any case, the ITU-R classifications are not essentially adequate assignments. From this work, the precipitation rate values at diverse rates of time for numerous areas of Ethiopia don't compare to ITU-R classifications.

4.5 Specific Rain Attenuation on Terrestrial Line-of-Sight Links

4.5.1 Determination of specific rain attenuation

From figure 4.10 and 4.11 it is clearly seen that, the values of specific rain attenuation for the wave that was horizontal polarization has bigger value than for the wave vertical polarized. This is due to the raindrops have a shape of non-spherical whic has flattened base and Hence, the horizontally polarized waves are are more likely attenuated than the vertically polarized waves.

From figure 4.10 and 4.11 it is additionally seen the particular rain attenuation for flat polarization is higher than for vertical polarization, since of the reality that the raindrops have a non-spherical shape with straightened base and so, the wave that polarized horizontally are more likely attenuated than the wave that ploarized vertically.

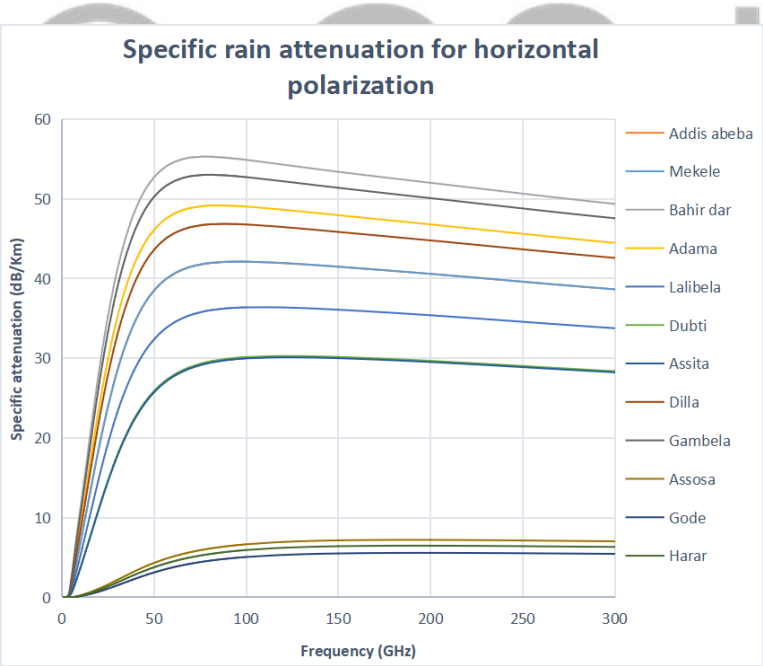

Figure 4.10: Specific rain attenuation for horizontal polarization

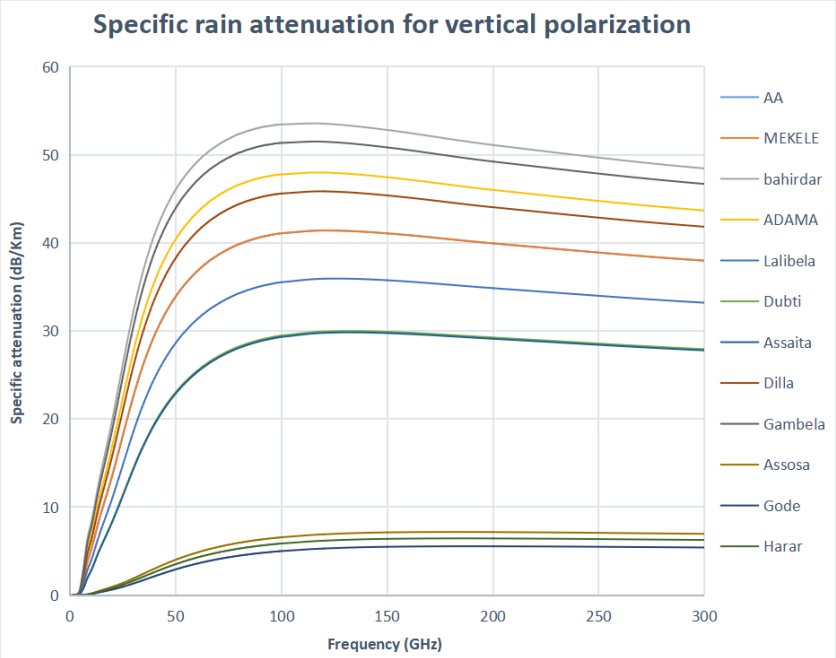

Figure 4.11: Specific rain attenuation for vertical polarization

4.5.2 Specific rain attenuation comparison

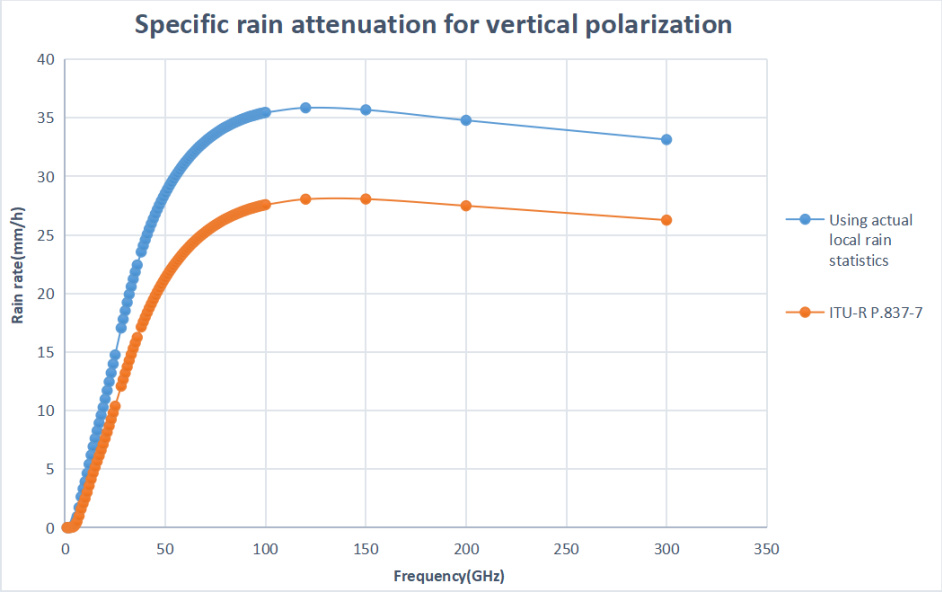

Figure 4.12: Specific rain attenuation for vertical polarization in Jimma; taking rain Rate exceeded for 0.01% of the time

Table 4.5: Values by which the ITU-R under –estimate the specific rain attenuation for Jimma)

Frequency(GHz)	New estimate specific rain Attenuation(dB/km)at VP	
	Local data	ITU-R P.837-7
10	3.92	2.49
20	10.97	7.61
30	18.5	13.19

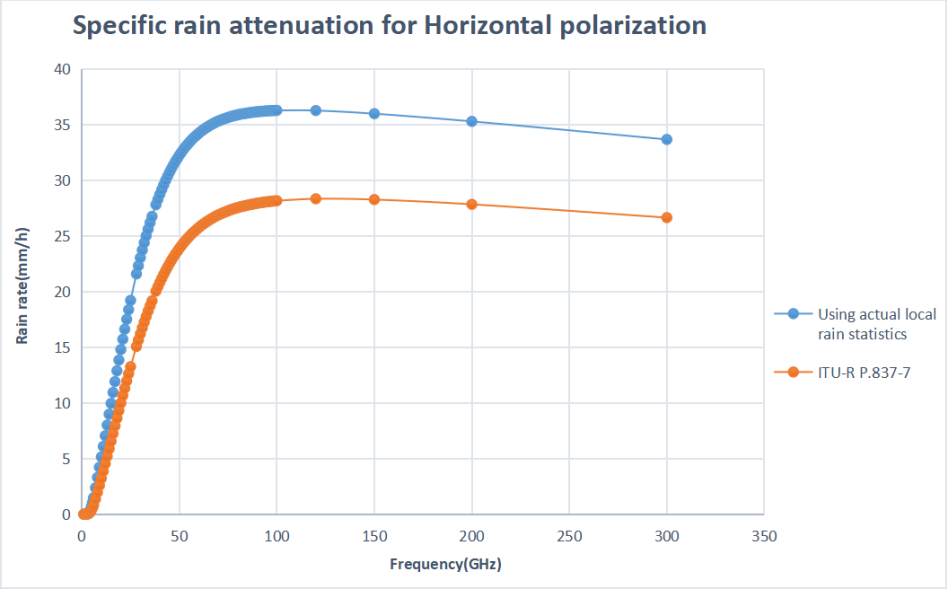

Figure 4.13: Specific rain attenuation for horizontal polarization in Jimma; taking rain Rate exceeded for 0.01% of the time

Table 4.6: Values by which the ITU-R under –estimate the specific rain attenuation for Jimma)

Frequency(GHz)	New estimate specific rain Attenuation(dB/km)at Hp	
	Local data	ITU-R P.837-7
10	5.15	3.23
20	14.8	9.99
30	23.05	16.2

The specific attenuation for both polarization that calculated depending on the locally measured rain rate exceeded for 0.01% was a higher than the specific attenuation that computed based on the rain rate that obtained from ITU-R P.837-7.

From the above figures 4.12 and 4.13, it is determined that the ITU-R average rain rate information applied to compute the particular rain attenuation beneath-expected the values of the rain attenuation while in comparison with the real local rain information measured at Jimma. It is visible that ITU-R prediction below-expected it. Looking at all, it may be conclusively said that these ITU-R designations aren't necessarily adequate. As referred to in advance, an adequate estimate of rain attenuation are normally derived from the available statistics on rain rates determined within the geographical location taken into consideration.

it's also located that, considerable rain attenuation turns into major among 5 GHz to 7 GHz upwards. Looking at frequencies under 5 GHz, the variations within the particular rain attenuation and that of the ITU-R aren't so conspicuous, which corroborates the earlier declaration through Moupfouma[30]that the occurrence of rainfall on radio hyperlinks within the tropical regional(equatorial weather in particular) becomes essential for frequencies as little as 7 GHz.

4.6 Specific Attenuation Contour Mapping for Ethiopia at 11GHz and 27GHz

As a part of the efforts to make certain minimal interference of wireless network service via rainfall events, radio hyperlinks design should accurately cope with signal deterioration at microwave and millimeter bands, particularly in tropical and equatorial areas in which Ethiopia is located. Therefore, it is imperative to develop contour maps from ITU recommendations at 99.99% link availability, for terrestrial link deployments across Ethiopia. In line with this, particular attenuation was at first computed for different locations at rain rate exceedences of 0.1% and 0.01% of time. Thereafter, results from these computations were exported to ArcGIS® software to generate contour maps, which demonstrate the spatial variation of specific attenuation over Ethiopia.

To this end, rainfall specific attenuation contour maps have been produced for the entire country for the design of future radio links operating at carrier frequency bands (11 GHz) and (27 GHz). These bands are exceedingly susceptible to rain constriction impact, however they present extraordinary opportunities within the future for network operators, because of their channel capacity for larger carrier bandwidths required to meet the growing traffic demand of wireless services. Generated contour maps for the required rain fade margin to mitigate rain attenuation at 0.01% are presented for 11GHz and 27GHz bands in below figures. For each figure, a set of contour maps showing vertical and horizontal polarization at each bands are available. Dataset used for this nationwide mapping considers the entire 60 locations in Ethiopia investigated in this work.

From results in Figure 4.14(a) and 4.14(b), it observed that in the Western, North-western and South-western parts of Ethiopia where heavy rainfall is prevalent, predicted specific attenuation for 11 GHz at 0.01% exceedance varies from 7.6 to 8.6 dB/km for vertically polarization; and 10.16 to 11.34 dB/km for horizontally polarized links. In central Ethiopia, specific attenuation values at 0.01% exceedance ranges from 4.92 to 5.81 dB/km for vertically polarized paths; and from 6.6 to 7.78 dB/km for 11 GHz horizontally polarized links. Towards the Eastern regions, where lower rainfall is experienced, specific attenuation values are also lower, ranging between 0.88 to 2.64 dB/km for vertically polarized paths; and 1.18 to 3.54dB/km for horizontally polarized paths. Applying this same analysis to Figure 4.15(a) and 4.15(b), the same trends are observed but with higher specific attenuation values since the carrier frequency is slightly higher at 27 GHz. Again, at the Western, North-western and South-western parts of Ethiopia, specific attenuation for 27 GHz at 0.01% exceedance varies from 22.75 to 25.44 dB/km for vertically polarization; and 30.06 to 33..61 dB/km for horizontally polarized paths. In central Ethiopia, specific attenuation values at 0.01% exceedance varies from 17.36 to 20.05 dB/km for vertically polarized

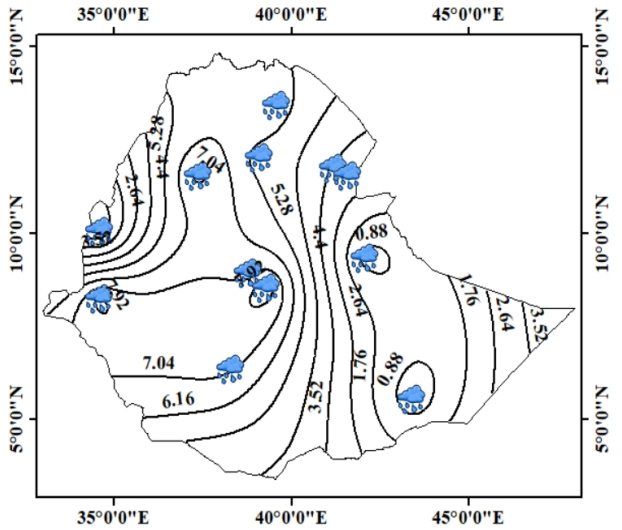

(a) Rain specific attenuation contour map for link at 27 GHz frequency at Vertical polarization

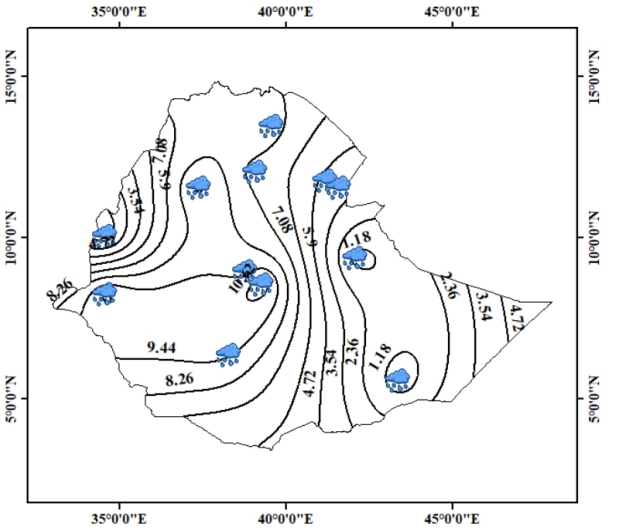

(b) Rain specific attenuation contour map for link at 27 GHz frequency for link availability of 0.01% in Ethiopia at Horizontal polarization

Figure 4.14: Rain specific attenuation contour map for link at 11 GHz frequency at Horizontal and vertical polarization

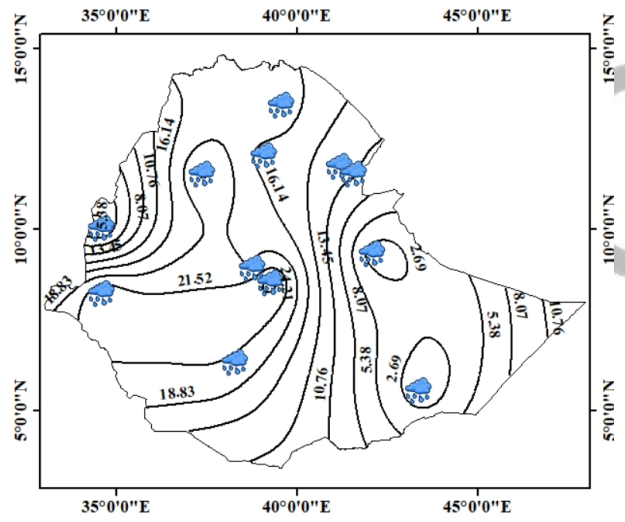

(a) Rain specific attenuation contour map for link at 27 GHz frequency at Vertical polarization

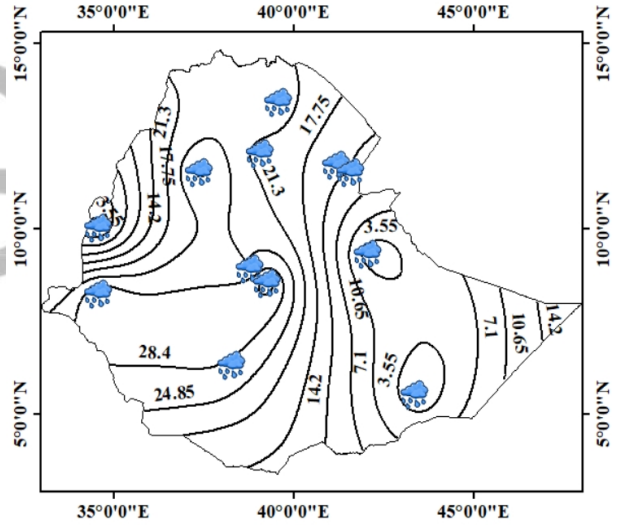

(b) Rain specific attenuation contour map for link at 27 GHz frequency at Horizontal polarization

Figure 4.15: Rain specific attenuation contour map for link at 27 GHz frequency for link availability of 0.01% in Ethiopia at Horizontal and vertical polarization

paths and from 22.94 to 26.94 dB/km for horizontally polarized paths.

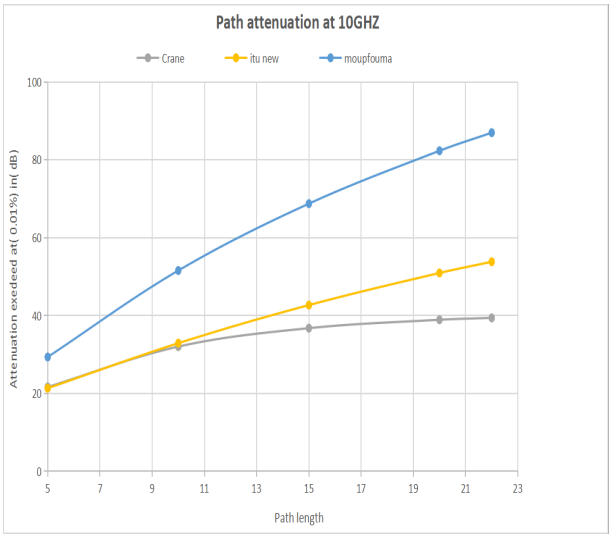

(a) Rain attenuation prediction models for terrestrial line-of-sight links for Addis Ababa for frequencies at 10 GHz

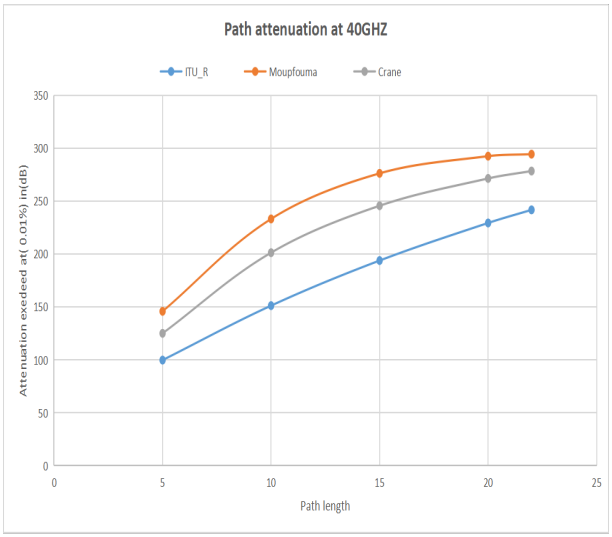

(b) Rain attenuation prediction models for terrestrial line-of-sight links for Addis Ababa for frequencies at 40 GHz

Figure 4.16: Rain attenuation exceeded for 0.01% of the time for Addis Ababa at 10 GHz and 40 GHz

4.7 Estimation and Comparison of Path Attenuation Using Different Existing Models on the Available Local Rain Data

In this section, an estimation of the path attenuation on a line-of-sight (LOS) is calculated using existing models based on the value of R0.01.

In conclusion, it is proved that these existing model results differently from each other. In addition, it may be observed that these behaviors depend on the values of years of rain rate data, the operating frequencies of the radio link, the link path distance and other factors of propagation measurements. ITU-R, which has the lowest attenuation, data on all possible topography locations in Ethiopia at higher frequency.

In the rain-attenuation estimation in northwest of Ethiopia is larger and inferior within the southeast part. Therefore, system designers must bear of those changes because they represent an unpredictability within the design of every radio link. The uncertainty could result in an over-cost, which will result to initial expenses and in long term periodic expenses. Also, as the instrument and getting higher (dB) values in some radio link mostly affects network availability and may cause service unavailability of communications link. Hence, It is important to make necessary changes for the differences via RF equipment modifications. The overall effects of those modifications are going to be seen within the service price.

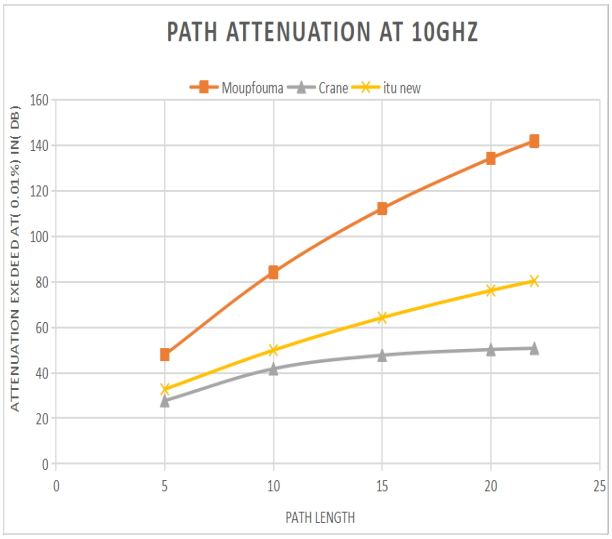

(a) Rain attenuation prediction models for terrestrial line-of-sight links for Bahirdar for frequencies at 10 GHz

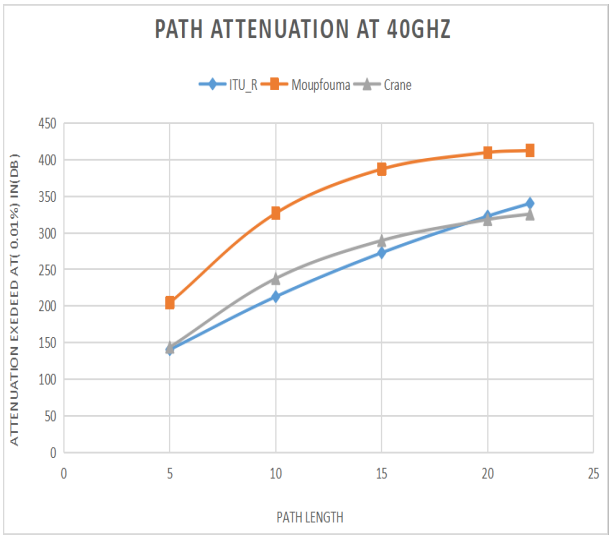

(b) Rain attenuation prediction models for terrestrial line-of-sight links for Bahirdar for frequencies at 40 GHz

Figure 4.17: Rain attenuation exceeded for 0.01% of the time for Bahirdar at 10 GHz and 40 GHz

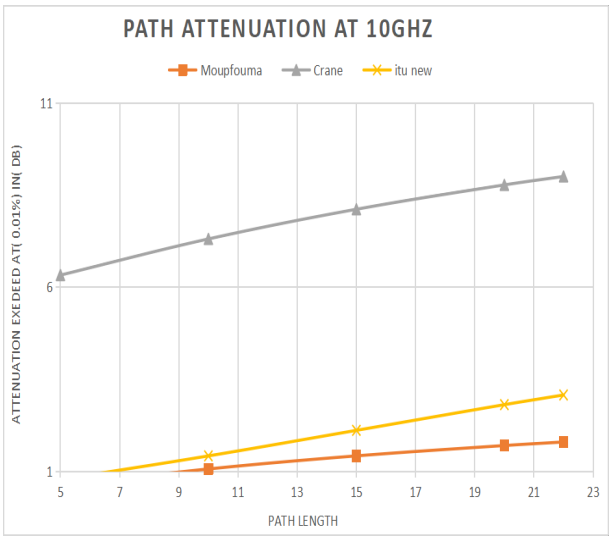

(a) Rain attenuation prediction models for terrestrial line-of-sight links for Gode for frequencies at 10 GHz

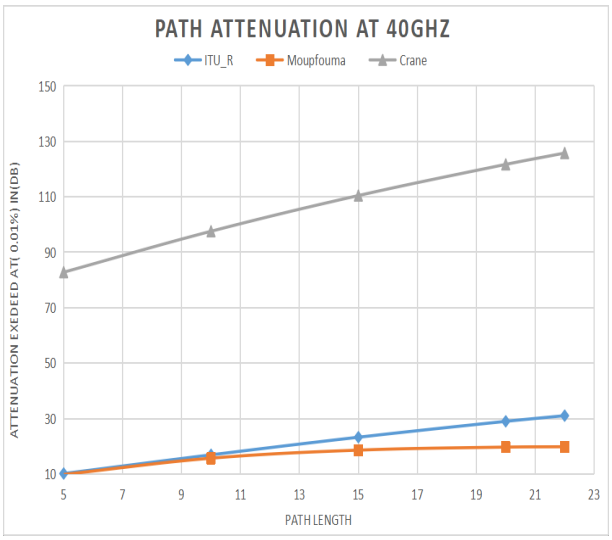

(b) Rain attenuation prediction models for terrestrial line-of-sight links for Gode for frequencies at 40 GHz

Figure 4.18: Rain attenuation exceeded for 0.01% of the time for Gode at 10 GHz and 40 GHz

The most takeaway point from the discussion so far has been the requirement to develop attenuation prediction models for an Ethiopian region are necessary. Models devised using rain attenuation models and experimental statistics of other regions of the world cannot produce reliable attenuation prediction results. This directly damage the service availability and customer experience. The network components, thus designed will not be able to give the necessary service required of them. The research work has tried to show attenuation statistics determination based on local rain rate values that represent the geographic locations under investigation.

4.8 Prediction of Rain Attenuation Model for Ethiopia from Measurements

4.8.1 Description of the link profile

Terrestrial Line-of-Sight radio link was found between Addis Ababa at a precise azimuthal angle of 203.92^o with an elevation of 2401 m above sea level and the site found at Furi is with an azimuthal angle of 23.910^o with elevation of 2842 m above sea. The radio link was using vertical polarization at a frequency of 11 GHz. The height above the ground was clear enough to see the path profile of figure 4.19(a) for the radio propagation network.

The performance analysis of line-of-sight radio link was considered depending on the analysis of the link budget formula. The link budget consideration includes the calculation of received signal value and fade margin. Therefore, Calculating for the power received P_r

$$P_r = P_t + G_{tx} + G_{rx} - FSL - L \tag{4.2}$$

Where, Where,P_t is the transmitting signal of the output power found at the transmitter Antenna input. This is the value of the radio link carrier power, most of the time this value is expressed in dBm
L is atmospheric gas loss, vegetation loss, buildings, loss due to clouds and fogs G_{tx} = is expressed as transmit antenna gainG_{rx} = is expressed as receive antenna gain FSL = Free space loss
Therefore, P_r= 30+42+42-139.6-0.9-6.8-0.35
P_r= -33.66dBm

The percentage amount of time where the radio wave signal below the limit of the receiver relative to the whole propagation time could describe the performance of a radio link. Therefore, the calculation of fade margin, the difference of receiving nominal signal value and receive threshold signal level, has to be analyzed:

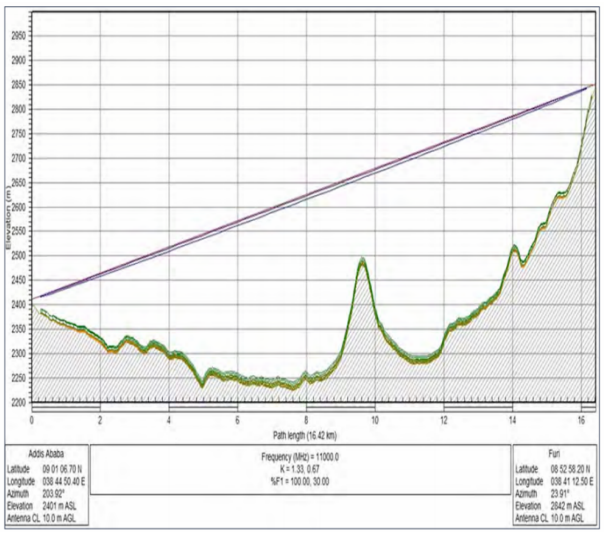

(a) Path profile for 16.42 km terrestrial line-of- sight link between Furi and Addis Ababa

Parameters	link	
	Addis Ababa	Furi
Elevation (m)	2401	2842
Latitude	09.01067^0N	08.52582^0N
Longitude	038.44504^0E	038.41125^0E
Antenna height(m)	10	10
Antenna gain (dBi)	42	42
Tx line unit loss(dB/100)	4.53	4.53
Tx line loss (dB)	0.91	0.91
Frequency(MHz)	11000	11000
Circuit branching loss (dB)	6.8	6.8
True azmuth (0)	203.92	23.91
Vertical angle	1.48	-1.59
Link distance (km)	16.42	
Free space loss (dB)	139.6	
Rx threshold level (dBm)	-76.2	
Effective frequency spacing (MHz)	21.7	
Atmospheric absorption loss (dB)	0.35	
Tx power (dBm)	30	

(b) link parameters for terrestrial line of sight networks

Figure 4.19: Description of the link profile

$$Fademargin = RSL - R_{XTH} \tag{4.3}$$

$Fademargin$= -33.66dBm - (-76.2dBm)= 42.54dB

Here, RSL is the received ammount of signal level and Rxth is the receiver minimum threshold. PR is designated as the received signal power which was calculated at the receiver end of the radio link. The transmitted power was 30 dBm and PR was calculated to be -33.66 for the radio link between Addis Ababa and Furi. If non-rainy time, which can cause attenuation, no losses absorbed. This is because of the absence of water vapour and fog, there is no multipath and diffraction fading. However, due to other types that could be reason of losses, the actual magnitude of signal at received side could be below this expected ideal value at both locations.

4.8.2 Non-rain faded signal level measurements

The measurements from the Non-rain faded signal values and the values of the corresponding 1-minute statistics were recorded in Addis Ababa for the year 2015, at July. The analysis has been made on the data. Then it was processed and the average values of the signal level from measurement for the non-rainy selected days of July was discovered. The below Figure illustrates the mean value of signal level for the selected particular non- rainy days. Where these could also be known as the non-rain faded mean values.

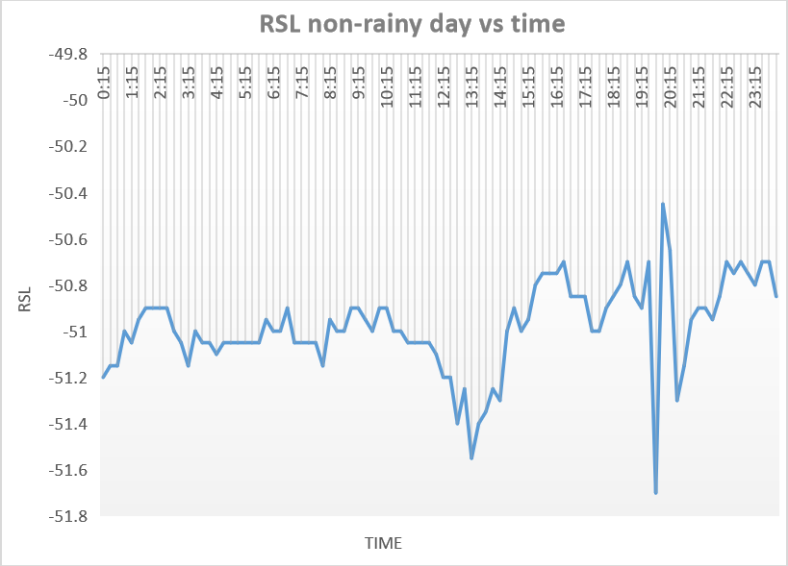

Figure 4.20: The received signal time series for Average non rainy days over 24 hours, July 2015

received signals resonate in values of -50.4 and -51.6dBm with the mean value of (-51dBm) for the selected particular days Non-rain Fade =-51-(-33.66) = -17.34dB
Therefore, the data from the signal attenuation, which was recorded in the month of JULY are estimated to be because of other factors. These are: foggy, obstructions, trees, vegetation and so on.

4.8.3 Calculation from rainy days data and its rain attenuation

This part also illustrates the measurement of rain rate versus the time series. Which was shown over the preferred rainy days. As a result, the variable values of the received signal magnitude and the attenuation of the rain for the selected days are presented in this part.
From the figure rain attenuation calculation for rainy month (July) by subtracting the average non-rain, Faded Signal Level from the total average received signal level at this particular month.

Rain attenuation=(total average received signal level) - (non-rain faded average signal level)

4.8.4 Rain attenuation modeling in Addis Ababa at 11GHz from measurements using three existing methods

After analyze signal level measurement data for July in Addis Ababa with the 16.42 km, link at 11 GHz recorded in the year 2015 that recorded between the two radio transmitting paths and then to calculate the rain attenuation Using the three known methods, these are: ITU-R, Crane Global and the Moupfouma, are applied to 1min local rainfall data using a new conversion model. And also compared

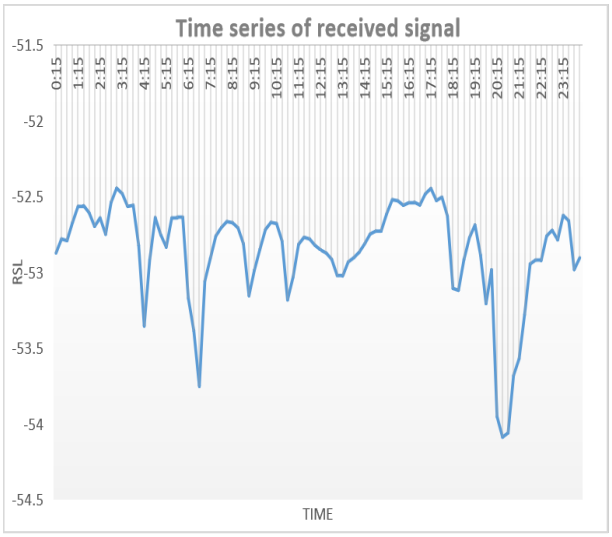

(a) The received signal time series for rainy days, July 2015

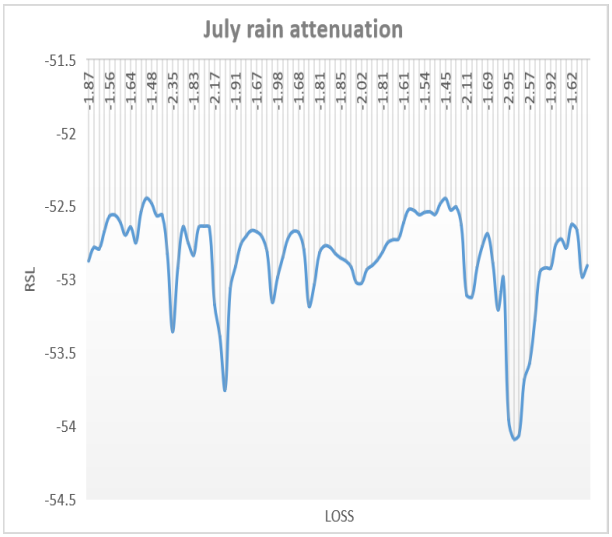

(b) Rain attenuation for rainy days, July 2015

Figure 4.21: Analysis of Rainy Days Data and Its Rain Attenuation

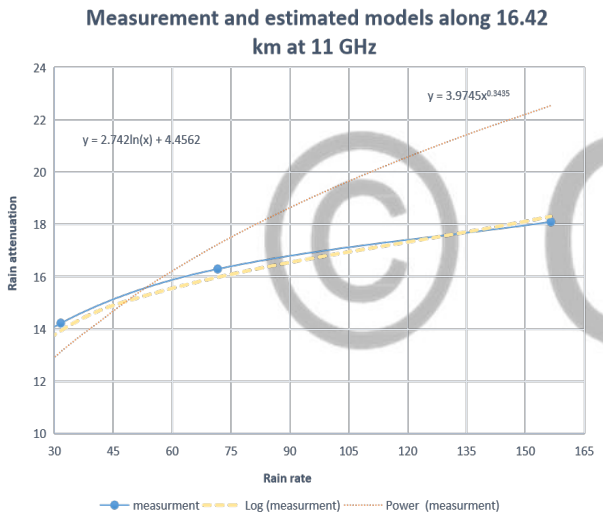

(a) Rain attenuation for Addis Ababa, 2015: Measurement and estimated models along 16.42 km at 11 GHz

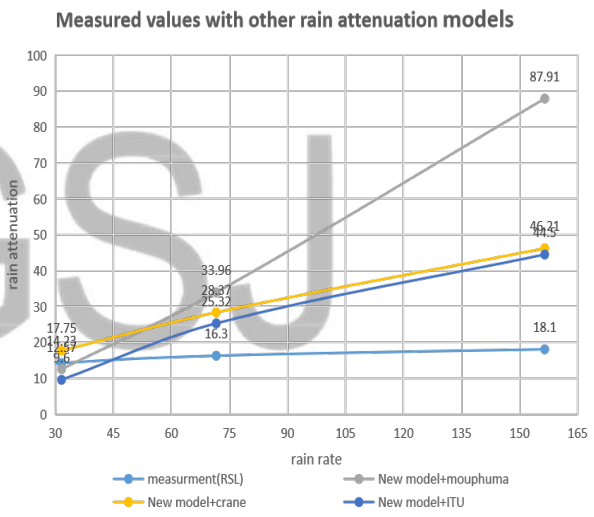

(b) Rain attenuation in Addis Ababa for July: Measurement and Models at 11 GHz

Figure 4.22: Analysis of Rainy Days Data and Its Rain Attenuation

with the actual attenuation from received signal level measurements. Logarithmic model and power estimation methods are then applied to fit the collected measured data. The Figure illustrates that modeling of rain attenuation in Addis Ababa from the actual measurements.

The figure 4.22(b) shows that the predicted rain attenuation models found for the July month in Addis Ababa at a frequency 11GHz from the practical measurements in relation to the previously known models. At this specific selected site and month, the attenuation predicted by new conversion model with ITU-R method has better attenuation estimation than other existing models. It is possible see the clear difference from this result for this specific location. If there are more links to be checked similarly with various distance and different frequency, it is possible to conclude as a country.

Chapter 5

Conclusion and Recommendation

5.1 Conclusion

The need of an accurate estimate of rainfall rate as well as rain attenuation found on terrestrial line-of-sight radio link at Micro and millimeteric wave frequency cannot be overemphasized in the study of radio communication. In this work, rain rate and prediction for Ethiopia have been examined and produced a new model of rain-induced attenuation. The Rain rate data collected over a period of 10 years (2000-2020) for 60 distinctive geological areas but for analysis to take 12 geographical location for the accurate prediction of rain rates statistics in Ethiopia.

In this work, integration time conversion was conducted based on Jimma data and the value obtained 122.9 mm/h has a huge difference compared to what global prediction methods would calculate. Yet, there is a strong requirement for accurate propagation prediction because of the fact that over-prediction could be ended up to costly over-design, on the other hand, under-prediction has a risk of unreliability to the systems. ITUR-P.837-7 calculates R0.01 for Jimma city as 84.76mm/h and new conversion model would make it around 118.88mm/h. These are difference, which lead to wrong design calculations if used. New conversion model conducted based on Jimma data was better prediction values were gained for other cities as well. For city of Bahirdar, for instance, ITU predicted R0.01 which is lower than that of Jimma when in fact it is known that Bahirdar experience the most intense of rain falls out of the major cities in Ethiopia. According to the conversion procedure used by this research work, the new R0.01 value is 225.44 mm/h. similar results are calculated for other major cities as well.

Subsequent conversion of rainfall data into equivalent one-minute rainfall rate statistics has assisted in the development of rain rate and rain specific attenuation contour maps for wireless radio links in Ethiopia. Results obtained have shown that ITU-R specification for R0.01 for terrestrial planning is much lower than the values obtained.However, the ITU-R approach of classifications is not essentially adequate. The precipitation values of rainfall-rate at various values of time for different areas of Ethiopia don't correspond to the values of ITU-R classifications.

Based on the simulation results, it can be concluded that: The specific attenuation based on the local data for horizontal polarization has more affected than the specific attenuation for vertical polarization; and the difference between these values was decreased with increase the operating frequency. The specific attenuation for horizontal polarization that calculated depending on the locally measured rain rate exceeded for 0.01% was a higher than the specific attenuation that computed based on the rain rate that

obtained from ITU-R P.837-5. The rain attenuation was increase with increase, at the path distance increase. The rain attenuation values decrease as the degree of availability decreases. At low percentage of a system availability of terrestrial link, the link can be ensured in the lower rain rate city like dubti, than the higher rain rate city like bahirdar. The results in this paper give a helpful information for engineers to design a terrestrial microwave link in Ethiopia.

5.2 Recommendation

The research and findings in this thesis can be advanced by considering the following points.

- IIt should be applied to other part of the country located in Ethiopia over a long period of years. This approach will in turn allow a much better accuracy to the rainfall-rate expectations.
- Determine rain rate profile is an important part of propagation studies concerned with rain. It is impossible to design reliable communication links without proper rain data and processing tools. Due to lack of measured 1-minute rain data for most of sites except Jimma, the research work has employed the best rain rate integration time conversion method from among the number of approaches. The conversion was based on 1-min and 15-min measured data collected for Jimma town. The approach could be seeking to get 1-min rain rate from 15-min integration rain rate data that is available from NMA. The researcher also believes the conversion mechanism can be improved if 1-min data could be collected for more sites investigation of rain effect on microwave and millimeter wave bands than just Jimma. So, future researchers, in a view to find better rain rate predictions, should base their studies on measured 1-min rain rate data.So, integrating with a smaller time gap of rain rate such as 10, 20, and 30 secs ought to be looked for after a much better approach of predicting rain attenuation models.
- The signal attenuation estimations should be used for more topographical areas in Ethiopia geography and this must be extended to cover a period of long time.

Bibliography

[1] MO Fashuyi, PA Owolawi, and TJ Afullo. "Rainfall rate modelling for LoS radio systems in South Africa". In: *Trans. of South African Inst. of Elect. Engineers (SAIEE)* 97.1 (2006), pp. 74–81.

[2] RP Series. "Propagation data and prediction methods required for the design of terrestrial line-of-sight systems". In: *Recommendation ITU-R* (2015), pp. 530–12.

[3] Qammer H Abbasi et al. "A novel pathloss model for angular and spatial dependency of ultra wideband off-body radio channels". In: *International Journal on Communications Antenna and Propagation* 3.4 (2013), pp. 206–209.

[4] Promise Elechi and Paul Osaretin Otasowie. "Comparison of empirical path loss propagation models with building penetration path loss model". In: *International Journal on Communications Antenna and Propagation (I. Re. CAP)* 6.2 (2016), pp. 116–123.

[5] Akintunde Ayodeji Alonge and Thomas Joachim Odhiambo Afullo. "Rainfall microstructural analysis for microwave link networks: Comparison at equatorial and subtropical Africa". In: *Progress In Electromagnetics Research* 59 (2014), pp. 45–58.

[6] Robert K Crane. *Electromagnetic wave propagation through rain*. Wiley-Interscience, 1996.

[7] PA Owolawi, SJ Malinga, and TJO Afullo. "Estimation of terrestrial rain attenuation at microwave and millimeter wave signals in South Africa using the ITU-R model". In: *PIERS Proceedings, Kuala Lumpur, Malaysia* (2012).

[8] Fashuyi Modupe Olubunmi. "A study of rain attenuation on terrestrial paths at millimetric wavelengths in South Africa." PhD thesis. 2006.

[9] MO Odedina and TJ Afullo. "Seasonal variations of rain attenuation on radio propagation paths in South Africa". In: (2008).

[10] MO Fashuyi, PA Owolawi, and TJ Afullo. "Rainfall rate modelling for LoS radio systems in South Africa". In: *Trans. of South African Inst. of Elect. Engineers (SAIEE)* 97.1 (2006), pp. 74–81.

[11] Fidèle Moupfouma. "Electromagnetic waves attenuation due to rain: A prediction model for terrestrial or LOS SHF and EHF radio communication links". In: *Journal of Infrared, Millimeter, and Terahertz Waves* 30.6 (2009), pp. 622–632.

[12] Zhen-wei Zhao, Ming-gao Zhang, and Zhen-sen Wu. "Analytic specific attenuation model for rain for use in prediction methods". In: *International Journal of Infrared and millimeter waves* 22.1 (2001), pp. 113–120.

[13] RP Series. "Propagation data and prediction methods required for the design of terrestrial line-of-sight systems". In: *Recommendation ITU-R* (2015), pp. 530–12.

[14] FC Medeiros Filho, RS Cole, and AD Sarma. "Millimetre-wave rain induced attenuation: theory and experiment". In: *IEE Proceedings H (Microwaves, Antennas and Propagation)*. Vol. 133. 4. IET. 1986, pp. 308–314.

[15] RL Olsen. "Radioclimatological modeling of propagation effects in clear-air and precipitation conditions: Recent advances and future directions". In: *Radio Africa* (1999), pp. 25–29.

[16] Mersha Eyob. "Adaptive code modulation for rainfall fade mitigation in Ethiopia". PhD thesis. ASTU, 2019.

[17] Feyisa Debo Diba. "Radio wave propagation modeling under precipitation and clear-air at microwave and millimetric bands over wireless links in the horn of Africa." In: 2017.

[18] Sujan Shrestha and Dong-You Choi. “Rain attenuation statistics over millimeter wave bands in South Korea”. In: *Journal of Atmospheric and Solar-Terrestrial Physics* 152 (2017), pp. 1–10.

[19] Sakir Hossain. “Rain attenuation prediction for terrestrial microwave link in Bangladesh”. In: *arXiv preprint arXiv:1406.5038* (2014).

[20] PA Owolawi, SJ Malinga, and TJO Afullo. “Estimation of terrestrial rain attenuation at microwave and millimeter wave signals in South Africa using the ITU-R model”. In: *PIERS Proceedings, Kuala Lumpur, Malaysia* (2012).

[21] Pius Adewale Owolawi. “Rainfall rate probability density evaluation and mapping for the estimation of rain attenuation in South Africa and surrounding islands”. In: *Progress In Electromagnetics Research* 112 (2011), pp. 155–181.

[22] GO Ajayi and EBC Ofoche. “Some tropical rainfall rate characteristics at Ile-Ife for microwave and millimeter wave applications”. In: *Journal of Applied Meteorology and Climatology* 23.4 (1984), pp. 562–567.

[23] SJ Malinga, PA Owolawi, and TJO Afullo. “Determination of specific rain attenuation using different total cross section models for Southern Africa”. In: *SAIEE Africa Research Journal* 105.1 (2014), pp. 20–30.

[24] MO Fashuyi, PA Owolawi, and TJ Afullo. “Rainfall rate modelling for LoS radio systems in South Africa”. In: *Trans. of South African Inst. of Elect. Engineers (SAIEE)* 97.1 (2006), pp. 74–81.

[25] Peter Odero Akuon and TJO Afullo. “Rain cell sizing for the design of high capacity radio link systems in South Africa.” In: *Progress In Electromagnetics Research B* 35 (2011).

[26] Akintunde Ayodeji Alonge and Thomas Joachim Odhiambo Afullo. “Rainfall microstructural analysis for microwave link networks: Comparison at equatorial and subtropical Africa”. In: *Progress In Electromagnetics Research* 59 (2014), pp. 45–58.

[27] SJ Malinga, PA Owolawi, and TJO Afullo. “Computation of rain attenuation through scattering at microwave and millimeter bands in South Africa”. In: *Progress in Electromagnetics Research Symposium Proceedings*. 2013, pp. 959–971.

[28] Kesavan Ulaganathen et al. “Comparative studies of the rain attenuation predictions for tropical regions”. In: *Progress In Electromagnetics Research M* 18 (2011), pp. 17–30.

[29] Sakir Hossain. “Rain attenuation prediction for terrestrial microwave link in Bangladesh”. In: *arXiv preprint arXiv:1406.5038* (2014).

[30] Fidele Moupfouma. “Improvement of a rain attenuation prediction method for terrestrial microwave links”. In: *IEEE Transactions on Antennas and Propagation* 32.12 (1984), pp. 1368–1372.

[31] Khandaker Lubaba Bashar and Mohammad Mahfujur Rashid. “Performance analysis of rain fades on microwave earth-to-satellite links in Bangladesh”. In: *Journal of Engineering and Technology* 4.7 (2014).

[32] VR Antti and Arto Lehto. *Radio engineering for wireless communication and sensor applications*. Artech house, 2003.

[33] Roger G Barry and Richard J Chorley. *Atmosphere, weather and climate*. Routledge, 2009.

[34] VR Antti and Arto Lehto. *Radio engineering for wireless communication and sensor applications*. Artech house, 2003.

[35] Philip F Panter. *Communication systems design: line-of-sight and tropo-scatter systems*. McGraw-Hill Companies, 1972.

[36] RP Series. “Propagation data and prediction methods required for the design of terrestrial line-of-sight systems”. In: *Recommendation ITU-R* (2015), pp. 530–11.

[37] Robert Crane. “Prediction of attenuation by rain”. In: *IEEE Transactions on communications* 28.9 (1980), pp. 1717–1733.

[38] Fidele Moupfouma. "Improvement of a rain attenuation prediction method for terrestrial microwave links". In: *IEEE Transactions on Antennas and Propagation* 32.12 (1984), pp. 1368–1372.

[39] JA Garcaa-Lopez and J Peiro. "Simple rain-attenuation-prediction technique for terrestrial radio links". In: *Electronics Letters* 19.21 (1983), pp. 879–880.

[40] Radiowave Propagation Series. "Characteristics of precipitation for propagation modelling". In: *Recommendation ITU-R* (2012), pp. 837–6.

[41] RP Series. "Characteristics of precipitationfor propagation modelling". In: *Recommendation ITU-R P.837-6* (2012).

[42] RP Series. "Propagation data and prediction methods required for the design of terrestrial line-of-sight systems". In: *Recommendation ITU-R* (2017), pp. 530–11.

[43] Khandaker Lubaba Bashar and Mohammad Mahfujur Rashid. "Performance analysis of rain fades on microwave earth-to-satellite links in Bangladesh". In: *Journal of Engineering and Technology* 4.7 (2014).

[44] SJ Malinga, PA Owolawi, and TJO Afullo. "Computation of rain attenuation through scattering at microwave and millimeter bands in South Africa". In: *Progress in Electromagnetics Research Symposium Proceedings*. 2013, pp. 959–971.

[45] Abiyu Kirubel. "Investigation of rain effect on MIMO Systems at microwave and millimeter wave bands". PhD thesis. ASTU, 2019.

[46] B Segal. "The influence of raingage integration time, on measured rainfall-intensity distribution functions". In: *Journal of Atmospheric and Oceanic Technology* 3.4 (1986), pp. 662–671.

[47] Augusto Burgueno, Manuel Puigcerver, and Enric Vilar. "Influence of rain gauge integration time on the rain rate statistics used in microwave communications". In: *annales des telecommunications*. Vol. 43. 9. Springer. 1988, pp. 522–527.

[48] J Chebil and TA Rahman. "Rain rate statistical conversion for the prediction of rain attenuation in Malaysia". In: *Electronics Letters* 35.12 (1999), pp. 1019–1021.

[49] JH Lee et al. "Conversion of rain rate distribution for various integration time". In: *IEEE Transactions on Microwave Theory and Techniques* 42.11 (1994), pp. 2099–2106.

[50] ROGERS Olsen, D V Rogers, and D Hodge. "The aR b relation in the calculation of rain attenuation". In: *IEEE Transactions on antennas and propagation* 26.2 (1978), pp. 318–329.

[51] RP Series. "Specific attenuation model for rain for use in prediction methods". In: *Recommendation ITU-R P.838-3* (2005).

[52] RP Series. "Conversion of annual statistics to worst-month statistics". In: *Recommendation ITU-R P.841-5* (2016).

[53] Shuo Wang et al. "Comparison of interpolation methods for estimating spatial distribution of precipitation in Ontario, Canada". In: *International Journal of Climatology* 34.14 (2014), pp. 3745–3751.

[54] Abdullah Konak. "A kriging approach to predicting coverage in wireless networks". In: *International Journal of Mobile Network Design and Innovation* 3.2 (2009), pp. 65–71.

[55] Yong Xiao et al. "Geostatistical interpolation model selection based on ArcGIS and spatio-temporal variability analysis of groundwater level in piedmont plains, northwest China". In: *SpringerPlus* 5.1 (2016), pp. 1–15.

[56] Margaret A Oliver and Richard Webster. "Kriging: a method of interpolation for geographical information systems". In: *International Journal of Geographical Information System* 4.3 (1990), pp. 313–332.

[57] Margaret A Oliver and Richard Webster. "Kriging: a method of interpolation for geographical information systems". In: *International Journal of Geographical Information System* 4.3 (1990), pp. 313–332.

[58] Chia-Yu Wu et al. “Comparison of different spatial interpolation methods for historical hydrographic data of the lowermost Mississippi River”. In: *Annals of GIS* 25.2 (2019), pp. 133–151.

Appendix A

Appendix 1: ITU-R Parameters for rainfall specific Attenuation Estimation

The ITU-R recommendation P.838-3 document gives the procedure for estimating the specific attenuation at different frequencies by applying two power-law coefficients, K and α. The independent parameter is given as the rainfall rate at 0.01% of the time, R0.01, which is regional dependent. Thus, The specific attenuation is given by:

$$A = K * R_{0.01}^{\alpha} \tag{A.1}$$

The values of k and α for horizontal and vertical polarization systems are thus presented:

Table A.1: ITU-R Parameters for rainfall specific Attenuation Estimation[51]

F(GHz)	KH	aH	KV	aV
1	0.0000259	0.9691	0.0000308	0.9691
1.5	0.0000443	1.0185	0.0000574	1.0185
2	0.0000847	1.0664	0.0000998	1.0664
2.5	0.0001321	1.1209	0.0001464	1.1209
3	0.000139	1.2322	0.0001942	1.2322
3.5	0.0001155	1.4189	0.0002346	1.4189
4	0.0001071	1.6009	0.0002461	1.6009
4.5	0.000134	1.6948	0.0002347	1.6948
5	0.0002162	1.6969	0.0002428	1.6969
5.5	0.0003909	1.6499	0.0003115	1.6499
6	0.0007056	1.59	0.0004878	1.59
7	0.001915	1.481	0.001425	1.481
8	0.004115	1.3905	0.00345	1.3905
9	0.007535	1.3155	0.006691	1.3155
10	0.01217	1.2571	0.01129	1.2571
11	0.01772	1.214	0.01731	1.214
12	0.02386	1.1825	0.02455	1.1825
13	0.03041	1.1586	0.03266	1.1586
14	0.03738	1.1396	0.04126	1.1396
15	0.04481	1.1233	0.05008	1.1233
16	0.05282	1.1086	0.05899	1.1086
17	0.06146	1.0949	0.06797	1.0949
18	0.07078	1.0818	0.07708	1.0818
19	0.08084	1.0691	0.08642	1.0691
20	0.09164	1.0568	0.09611	1.0568
21	0.1032	1.0447	0.1063	1.0447
22	0.1155	1.0329	0.117	1.0329
23	0.1286	1.0214	0.1284	1.0214
24	0.1425	1.0101	0.1404	1.0101
25	0.1571	0.9991	0.1533	0.9991
26	0.1724	0.9884	0.1669	0.9884
27	0.1884	0.978	0.1813	0.978
28	0.2051	0.9679	0.1964	0.9679
29	0.2224	0.958	0.2124	0.958
30	0.2403	0.9485	0.2291	0.9485
31	0.2588	0.9392	0.2465	0.9392
32	0.2778	0.9302	0.2646	0.9302
33	0.2972	0.9214	0.2833	0.9214
34	0.3171	0.9129	0.3026	0.9129
35	0.3374	0.9047	0.3224	0.9047
36	0.358	0.8967	0.3427	0.8967
37	0.3789	0.889	0.3633	0.889
38	0.4001	0.8816	0.3844	0.8816
39	0.4215	0.8743	0.4058	0.8743
40	0.4431	0.8673	0.4274	0.8673
41	0.4647	0.8605	0.4492	0.8605
42	0.4865	0.8539	0.4712	0.8539
43	0.5084	0.8476	0.4932	0.8476
44	0.5302	0.8414	0.5153	0.8414

F(GHz)	KH	aH	KV	aV
45	0.5521	0.8355	0.5375	0.8355
46	0.5738	0.8297	0.5596	0.8297
47	0.5956	0.8241	0.5817	0.8241
48	0.6172	0.8187	0.6037	0.8187
49	0.6386	0.8134	0.6255	0.8134
50	0.66	0.8084	0.6472	0.8084
51	0.6811	0.8034	0.6687	0.8034
52	0.702	0.7987	0.6901	0.7987
53	0.7228	0.7941	0.7112	0.7941
54	0.7433	0.7896	0.7321	0.7896
55	0.7635	0.7853	0.7527	0.7853
56	0.7835	0.7811	0.773	0.7811
57	0.8032	0.7771	0.7931	0.7771
58	0.8226	0.7731	0.8129	0.7731
59	0.8418	0.7693	0.8324	0.7693
60	0.8606	0.7656	0.8515	0.7656
61	0.8791	0.7621	0.8704	0.7621
62	0.8974	0.7586	0.8889	0.7586
63	0.9153	0.7552	0.9071	0.7552
64	0.9328	0.752	0.925	0.752
65	0.9501	0.7488	0.9425	0.7488
66	0.967	0.7458	0.9598	0.7458
67	0.9836	0.7428	0.9767	0.7428
68	0.9999	0.74	0.9932	0.74
69	1.0159	0.7372	1.0094	0.7372
70	1.0315	0.7345	1.0253	0.7345
71	1.0468	0.7318	1.0409	0.7318
72	1.0618	0.7293	1.0561	0.7293
73	1.0764	0.7268	1.0711	0.7268
74	1.0908	0.7244	1.0857	0.7244
75	1.1048	0.7221	1.1	0.7221
76	1.1185	0.7199	1.1139	0.7199
77	1.132	0.7177	1.1276	0.7177
78	1.1451	0.7156	1.141	0.7156
79	1.1579	0.7135	1.1541	0.7135
80	1.1704	0.7115	1.1668	0.7115
81	1.1827	0.7096	1.1793	0.7096
82	1.1946	0.7077	1.1915	0.7077
83	1.2063	0.7058	1.2034	0.7058
84	1.2177	0.704	1.2151	0.704
85	1.2289	0.7023	1.2265	0.7023
86	1.2398	0.7006	1.2376	0.7006
87	1.2504	0.699	1.2484	0.699
88	1.2607	0.6974	1.259	0.6974
89	1.2708	0.6959	1.2694	0.6959
90	1.2807	0.6944	1.2795	0.6944
91	1.2903	0.6929	1.2893	0.6929
92	1.2997	0.6915	1.2989	0.6915
93	1.3089	0.6901	1.3083	0.6901

F(GHz)	KH	aH	KV	aV
94	1.3179	0.6888	1.3175	0.6888
95	1.3266	0.6875	1.3265	0.6875
96	1.3351	0.6862	1.3352	0.6862
97	1.3434	0.685	1.3437	0.685
98	1.3515	0.6838	1.352	0.6838
99	1.3594	0.6826	1.3601	0.6826
100	1.3671	0.6815	1.368	0.6815
120	1.4866	0.664	1.4911	0.664
150	1.5823	0.6494	1.5896	0.6494
200	1.6378	0.6382	1.6443	0.6382
300	1.6286	0.6296	1.6286	0.6296
400	1.586	0.6262	1.582	0.6262
500	1.5418	0.6253	1.5366	0.6253
600	1.5013	0.6262	1.4967	0.6262
700	1.4654	0.6284	1.4622	0.6284
800	1.4335	0.6315	1.4321	0.6315
900	1.405	0.6353	1.4056	0.6353
1 000	1.3795	0.6396	1.3822	0.6396